Complex & Intelligent Systems (2022) 8:3161–3183
https://doi.org/10.1007/s40747-021-00563-y

ORIGINAL ARTICLE

Brain tumor detection and classification using machine learning: a comprehensive survey

Javaria Amin[1,2] · Muhammad Sharif[2] · Anandakumar Haldorai[3] · Mussarat Yasmin[2] · Ramesh Sundar Nayak[4]

Received: 28 July 2021 / Accepted: 12 October 2021 / Published online: 8 November 2021

Abstract

Brain tumor occurs owing to uncontrolled and rapid growth of cells. If not treated at an initial phase, it may lead to death. Despite many significant efforts and promising outcomes in this domain, accurate segmentation and classification remain a challenging task. A major challenge for brain tumor detection arises from the variations in tumor location, shape, and size. The objective of this survey is to deliver a comprehensive literature on brain tumor detection through magnetic resonance imaging to help the researchers. This survey covered the anatomy of brain tumors, publicly available datasets, enhancement techniques, segmentation, feature extraction, classification, and deep learning, transfer learning and quantum machine learning for brain tumors analysis. Finally, this survey provides all important literature for the detection of brain tumors with their advantages, limitations, developments, and future trends.

Keywords Brain imaging modalities · Segmentation · Feature extraction · MRI · Stroke

Introduction

The central nervous system disseminates sensory information and its corresponding actions throughout the body [1–3]. The brain, along with the spinal cord, assists in this dissemination. The brain's anatomy [4] contains three main parts; brain stem, cerebrum, and cerebellum. The weight of a normal human brain is approximately 1.2–1.4 K, with a volume of 1260 cm^3 (male brain) and 1130 cm^3 (female brain) [5]. The frontal lobe of brain assists in problem-solving, motor control, and judgments. The parietal lobe manages body position. The temporal lobe controls memory and hearing functions, and occipital lobe supervises the brain's visual processing activities. The outer part of cerebrum is known as cerebral cortex, and is a greyish material; it is composed of cortical neurons [6]. The cerebellum is relatively smaller than the cerebrum. It is responsible for motor control, i.e., systematic regulation of voluntary movements in living organisms with a nervous system. Due to variable size and stroke territory, ALI, lesionGnb, and LINDA methods fail to detect the small lesion region. Cerebellum is well-structured and well-developed in human beings as compared to other species [7]. The cerebellum has three lobes; an anterior, a posterior, and a flocculonodular. A round-shaped structure named vermis connects the anterior and posterior lobes. The cerebellum consists of an inner area of white matter (WM) and an outer greyish cortex, which is a bit thinner than that of the cerebrum. The anterior and posterior lobes assist in the coordination of complex motor movements. The flocculonodular lobe maintains the body's balance [4, 8]. The brain stem, as the name states, is a 7–10 cm-long stem-like structure. It contains cranial and peripheral nerve bundles and assists in eye movements and regulations, balance and maintenance, and some essential activities such as breathing. The nerve tracks originating from the cerebrum's thalamus pass through the brain stem to reach the spinal cord. From there, they spread throughout the body. The main parts of the brain stem are midbrain, pons, and medulla. The midbrain assists in functions such as motor, auditory, and visual processing, as well as eye movements. The pons assists in breathing, intra-brain

✉ Javaria Amin
javeria.amin@uow.edu.pk

1 Department of Computer Science, University of Wah, Wah Cantt, Pakistan

2 Department of Computer Science, COMSATS University Islamabad, Wah Campus, Islamabad, Pakistan

3 Department of Computer Science and Engineering, Sri Eshwar College of Engineering, Coimbatore, Tamil Nadu, India

4 Department of IS&E, Canara Engineering College, Mangaluru, Karnataka, India

communication, and sensations, and medulla oblongata helps in blood regulation, swallowing, sneezing, etc. [9].

Brain tumor and stroke lesions

Brain tumors are graded as slow-growing or aggressive [2, 10–20]. A benign (slow-growing) tumor does not invade the neighboring tissues; in contrast, a malignant (aggressive) tumor propagates itself from an initial site to a secondary site [16, 17, 21–27]. According to WHO, a brain tumor is categorized into grades I–IV. Grades I and II tumors are considered as slow-growing, whereas grades III and IV tumors are more aggressive, and have a poorer prognosis [28]. In this regard, the detail of brain tumor grades is as follows.

Grade I: These tumors grow slowly and do not spread rapidly. These are associated with better odds for long-term survival and can be removed almost completely by surgery. An example of such a tumor is grade 1 pilocyticastrocytoma.

Grade II: These tumors also grow slowly but can spread to neighboring tissues and become higher grade tumors. These tumors can even come back after surgery. Oligodendroglioma is a case of such a tumor.

Grade III: These tumors develop at a faster rate than grade II, and can invade the neighboring tissues. Surgery alone is insufficient for such tumors, and post-surgical radiotherapy or chemotherapy is recommended. An example of such a tumor is anaplastic astrocytoma.

Grade IV: These tumors are the most aggressive and are highly spreadable. They may even use blood vessels for rapid growth. Glioblastoma multiforme is such a type of tumor [29].

Ischemic stroke: Ischemic stroke is an aggressive disease of brain and it is major cause of disability and death around the globe [30]. An ischemic stroke occurs when the blood supply to the brain is cut off, resulting underperfusion (in tissue hypoxia) and dead the advanced tissues in hours [31]. Based on the severity, stroke lesions are categories into different stages such as acute (0–24 h), sub-acute (24 h–2 weeks) and chronic (>2 weeks) [32].

Brain imaging modalities

Three major methods (PET, CT, DWI and MRI) for brain tumors are widely used to analyze the brain structure.

Positron emission tomography

Positron emission tomography (PET) uses a special type of radioactive tracers. Metabolic brain tumor features such as blood flow, glucose metabolism, lipid synthesis, oxygen consumption, and amino acid metabolism are analyzed through PET. It is still considered as one of the most powerful metabolic techniques and utilizes the best nuclear medicine named as fluorodeoxyglucose (FDG) [33]. FDG is a widely used PET tracer in brain images. Nevertheless, FDG-PET images have limitations, e.g., an inability to differentiate between necrosis radiation and a recurrent high-grade (HG) tumor [34]. Moreover, during a PET scan, radioactive tracers can cause harmful effects to the human body, causing a post-scan allergic reaction. Some patients are allergic to aspartame and iodine. In addition, PET tracers do not provide accurate localization of anatomical structure, because they have a relatively poor spatial resolution as compared to an MRI scan [35].

Computed tomography

Computed tomography (CT) images provide more in-depth information than images obtained from normal X-rays. The CT scan has received widespread recommendation and adoption since its inception. A study [36] determined that in the USA alone, the annual CT scan rate is 62 million, with 4 million for children. CT scans show soft tissues, blood vessels, and bones of different human body parts. It uses more radiation than normal X-rays. This radiation may increase the risk of cancers when multiple CT scans are performed. The associated risks of cancers have been quantified according to CT radiation doses [37, 38]. MRI can even help in evaluating structures obscured in a CT scan, and provides high contrast among the soft tissues, providing a clearer anatomical structure [39].

Magnetic resonance imaging

An MRI scan is used to completely analyze different bodyparts, and it also helps to detect abnormalities in the brain at earlier stages than other imaging modalities [40]. Hence, complex brain structures make tumor segmentation a challenging task [41–47]. This review discusses preprocessing approaches, segmentation techniques [48, 49], feature extraction and reduction methods, classification methods, and deep learning approaches. Finally, benchmark datasets and performance measures are presented.

Diffusion weighting imaging

MRI sequences are utilized to analyze the stroke lesions based on the several parameters such as age, location and extent regions [50]. In the context of treatment, a computerized method might be utilized for accurate diagnosis of the disease progression rate [51]. The neuroscientists of cognitive, who frequently conduct research in which cerebral impairments are linked to cognitive function They observed

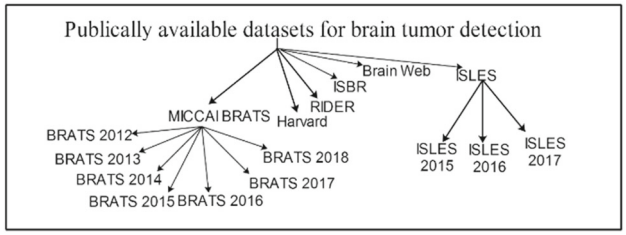

Fig. 1 Datasets for brain tumor detection

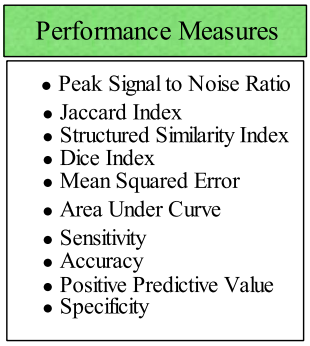

Fig. 2 List of performance measures for evaluation of brain tumor

that segmentation of the stroke lesions is a vital task to analyze the total infected region of brain that provide help in the treatment process [52]. However, segmentation of the stroke lesions is a difficult task, because stroke appearance is change as the passage of time. The MRI sequence such as diffusion weighted imaging (DWI) and FLAIR are utilized for stroke lesions detection. In acute stoke stage DWI sequence highlight the infection part as a hyperintensity. The underperfusion region represents the mapping magnitude of the perfusion [53]. The dis-similarity among two regions might be considered as penumbra tissue. Stroke lesions appear in distinct locations and shapes. Different types of lesions are appeared in a variable size and shape and these lesions are not aligned with vascular patterns and more than one lesions might appeared on similar time. The size of the stroke lesions is in radii of the few millimeters and appears in a full hemisphere. The structure of the hemisphere is dissimilar, and its intensity might significantly vary within the infected region. Furthermore, automated stroke segmentation is difficult due to the similar appearance of the pathology such as white matter hyperintensities and chronic stroke lesions [54].

Evaluation and validation

In the existing literature, experimental results are evaluated on publicly available datasets to verify the robustness of algorithms.

Publicly available datasets

Several datasets are publicly available that are used by the researchers to evaluate the proposed methods. Some important and challenging datasets are discussed in this section. BRATS are the most challenging MRI datasets [55–57]. BRATS Challenge is published in different years with more challenges having 1 mm^3 voxels resolution. The detail of datasets is given in Fig. 1 as well as in Table 1.

Performance metrics

The performance measures play a significant role to compute the method's effectiveness. A list of performance metrics is provided in Fig. 2.

Preprocessing

Preprocessing is a critical task [61] to extract the requisite region. 2D brain extraction algorithm (BEA) [62], FMRIB software library [63], and BSE [64] are used for non-brain tissue removal as shown in Fig. 3. The bias field is a key problem that arises in MRI due to imperfections of radio frequency coil called intensity inhomogeneity [65, 66]. It is corrected as shown in Fig. 4 [67]. The preprocessing methods like linear, nonlinear [68], fixed, multi-scale, and pixel-based are used in distinct circumstances [69–72]. The small variations among normal and abnormal tissues due to noise [68] and artifacts often provide difficulty in direct image analysis [73, 74]. AFINITI is used for brain tumor segmentation [63]. Consequently, automated techniques are adopted in which computer software performs segmentation and eliminates the need for manual human interaction [75, 76]. Fully and semi-automated techniques are used widely [77, 78]. The results of brain tumor segmentation are mentioned in Table 2. The segmentation methods are divided into the following categories.

- Conventional methods.
- Machine learning methods.
- Different inhomogeneities related to MRI noise have shading artifacts and partial volume effects.

When different types of tissues [61] take the same pixel, then it is called partial volume effect [92]. The random noise related to MRI [19, 93, 94] has Rician distribution [95]. In the literature, different filters such as wavelet, anisotropic diffusion, and adaptive are presented to enhance edges [96].

Table 1 Summary of the publicly available datasets

Datasets	Description	Sequences	Number of slices (images)
BRATS series	BRATS 2012 challengeimage (Patients) dataset (05 LGG, 10 HGG) casesSyntheticdataset (04 LGG,11HGG) cases	T1weighted, T1C weighted, T2 weighted and Flair	240 × 240 × 155
	BRATS 2012 Trainingimage dataset (10 LGG, 20 HGG) casesSyntheticdataset (25 LGG, 25 HGG) cases		
	BRATS 2013 challenge30 Subjects		
	BRATS 2013 Leaderboard, 25 Subjects		
	2014 challenge, 400 Subjects		
	2015 challenge, 274 Subjects		
	2016 challenge, Training cases of BRATS 2015		
	BRATS 2017 challenge, 285 Subjects		
	BRATS 2018 challenge, 191 Subjects		
	BRATS 2019 challenge, 22,087 training and 22,087 testing slices		
	BRATS 2020 challenge, 25,962 training and 25,962 testing slices		
Harvard [58]	65 tumor and 35 non-tumor images	T2 weighted	256 × 256 (100 images)
RIDER[59]	126 Subjects	T1 weighted, T2 weighted, and Flair	256 × 256 126 cases
ISLES 2015	64 Subjects	SISS- ISLES DWI, T1 weighted, T2 weighted, Flair SPES-ISLES CBF, CBV, DWI, T1C weighted, T2 weighted, Tmax, TTP	SISS- ISLES 230 × 230 × 154 (154 slices in each case) SPES-ISLES 230 × 230 × 154 (154 slices in each case)
ISLES 2016	75 Subjects	MTT, rCBV, relative rCBF, Tmax, TTP	192 × 192 × 19 (19 slices in each case)
ISLES 2017[60]	57 Subjects	PWI, ADC, MTT, rCBV, rCBF, Tmax, TTP	192 × 192 × 19 (19 slices in each case)

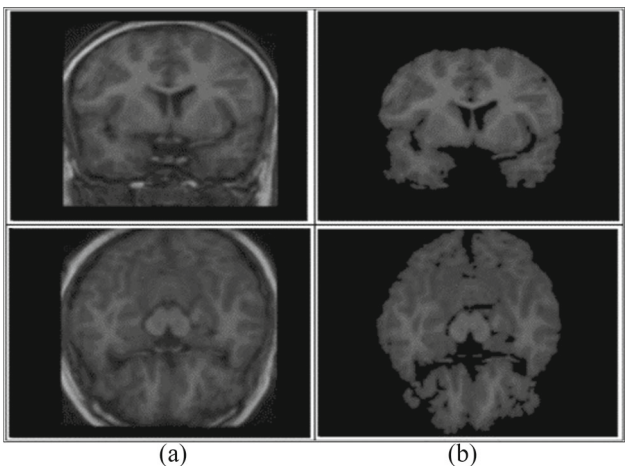

Fig. 3 Skull removal **a** input, **b** skull removed [1]

An anisotropic diffusion filter is more suitable in practical applications due to low computational speed [97, 98]. When the noise level is high in the image, it is difficult to recover the edges [99]. Normalizing the image intensity is another part of the preprocessing phase [2, 100, 101] and modified curvature diffusion equation (MCDE) [102] are applied for intensity normalization. Wiener filter is used to enhance the local and spatial information in medical imaging [103]. The widely utilized preprocessing methods are N4ITK [104] for the correction of bias field, median filter [104] for image smoothing, anisotropic diffusion filter [105], image registration [106], sharpening [107], and skull stripping through brain extraction tool (BET) [108].

Conventional methods

The conventional methods [46] are further categorized into the following:

- Thresholding methods.
- Region growing methods.
- Watershed methods.

Table 2 Summary of the existing segmentation approaches

References	Year	Segmentation methods	Datasets	Outcomes
[79]	2005	Hybrid level set (HLS) segmentation	10 patients	79.12 to 93.25% matching (PM)
[78]	2013	A semi-automatic method based on individual and population information	137 clinical images	94.1 ± 3.0 DSC
[80]	2015	Fully automated generative method	BRATS (2013 Challenge, 2013 Leaderboard, 2015 Challenge)	0.87 DSC complete, 0.82 core, 0.70 enhance on BRATS 2013 Challenge, 0.83 complete, 0.71 core, 0.54 enhance on BRATS 2013 Leaderboard, 0.81 DSC complete, 0.68 core DSC, 0.65 DSC enhance on BRATS 2015 Challenge
[81]	2016	Expectation maximization	SPES and SISS 2015	0.78 ± 0.08 DSC on SPES and 0.53 ± 0.26 DSC on SISS
[82]	2017	Otsu algorithm	BRATS 2013 Synthetic	0.93 ± 0.04 DSC on HG, 0.90 ± 0.02 DSC on LG 0.87 ± 0.06 Jaccard Index on HG, 0.82 ± 0.04 Jaccard Index on LG
[83]	2017	Non-negative matrix factorization (NMF)	21 HGG patients	0.80 complete DSC, 0.74 core DSC and 0.65 active DSC tumor
[84]	2017	HCSD	BRATS2012 Challenge	0.9102 ± 0.0627 DSC, 0.9501 ± 0.0518 SE, 0.9980 ± 0.0023 SP
[85]	2018	Improved thresholding method	Harvard and Private collected images	0.948 Jaccard index on clinical and 0.961 Jaccard index on Harvard
[86]	2018	Novel saliency method	BRATS 2013 Challenge	0.86 ± 0.06 HG DSC, 0.85 ± 0.07 LG DSC
[87]	2018	BA and RG	BRATS 2015 Challenge	0.8741 Jaccard index, 0.9036 DSC, 0.9827 sensitivity, 0.9772 specificity, 0.9753 accuracy and 0.9585 precision
[88]	2019	EM and FODPSO	192 MRI scan	0.93.4 ACC
[89]	2019	Adaptive threshold and morphological operations	1340 Clinical MR images	0.85 DSC, 0.89 Jaccard index
[90]	2020	3D semantic segmentation	BRATS 2019 challenge	0.826 enhance, 0.882 complete, 0.837 core tumor
[91]	2021	CNN model	FLAIR, (T1T1C, and T2) weighted	0.957 ACC

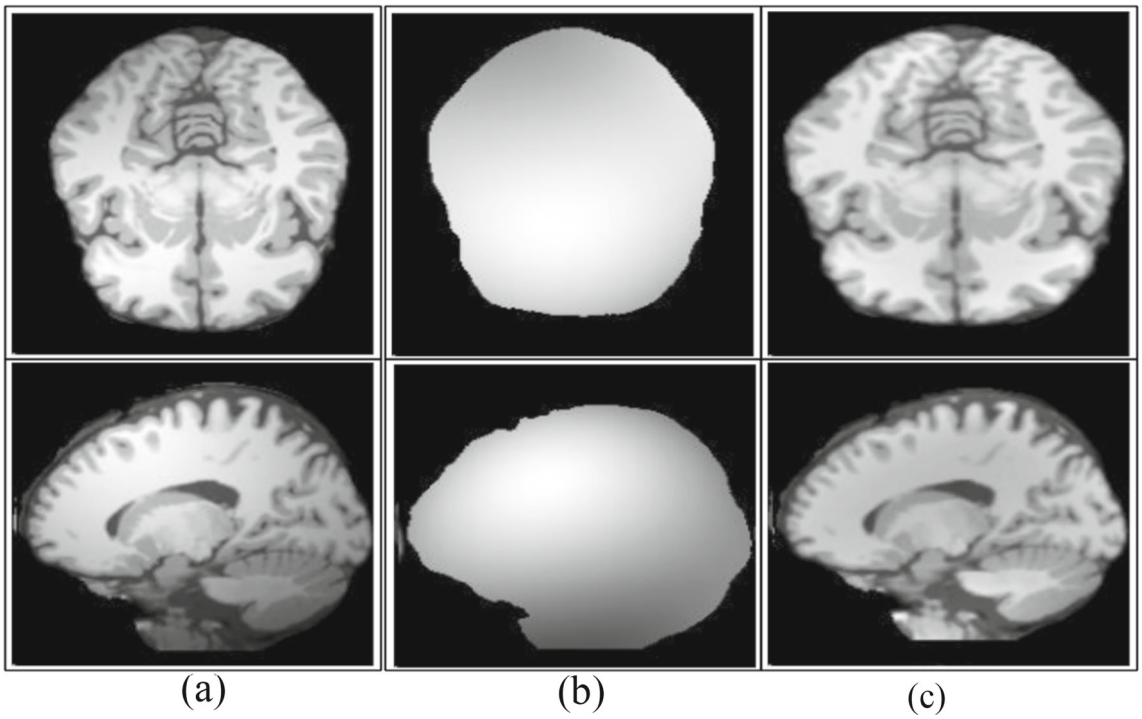

Fig. 4 Bias field correction **a** input, **b** estimated, **c** corrected [67]

Segmentation

Segmentation extracts the required region from input images. Thus, segmenting accurate lesion regions is a more crucial task [109]. As manual segmentation process is erroneous [110]; therefore, semi- and fully automated methods are utilized [46]. Segmentation of tumor region using semi-automated methods achieves acceptable outcomes over manual segmentation [111, 112]. Semi-automated methods are further divided into three forms: initialization, evaluation, and feedback response [113, 114].

Thresholding methods

The thresholding method is a basic and powerful method to segment the required objects [18] and the selection of an optimized threshold is a difficult task in low-contrast images. Histogram analysis is used to select threshold values based on image intensity [115]. Thresholding methods are classified into local and global. If high homogeneous contrast or intensity exists among the objects and background, then the global thresholding method is the best option for segmentation. The optimal threshold value can be determined by Gaussian distribution method [116]. These methods are utilized when the threshold value cannot be measured from the whole image histogram or single value of the threshold does not provide good results of segmentation [117]. In most cases, the thresholding method is applied at the first stage for segmentation and many distinct regions are segmented within the gray-level images as shown in Fig. 5.

Region growing (RG) methods

In RG approaches, image pixels form disjoint areas are analyzed through neighboring pixels, which are merged with homogeneousness characteristics based on pre-defined similitude criteria. The region growing might fail to provide better accuracy due to the partial volume effect [118, 119]. To overcome this effect, MRGM is preferred [86, 120]. The region growing with BA methods is also introduced [87].

Watershed methods

As MR images have more proteinaceous fluid intensity, therefore, watershed methods are utilized to analyze the intensity of the image [114, 121, 122]. Due to noise [123], watershed method leads to over-segmentation [124]. The accurate segmentation [125] results can be obtained by the combination of watershed transform with the merging of statistical methods [126, 127]. Some watershed algorithms are topological watershed [128], image foresting transform (IFT) watershed [129], and marker-based watershed [130].

The comprehensive literature review [131] on brain tumor detection shows that there is room for improvement [72]. As a brain tumor appears in variable sizes and shapes, existing segmentation approaches require additional improvements

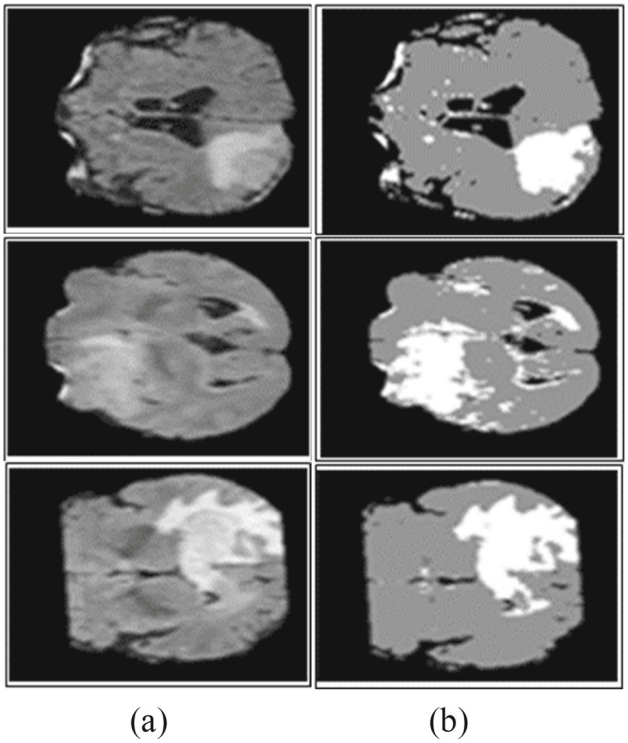

Fig. 5 Segmentation using Otsu thresholding **a** original images, **b** Otsu thresholding [82]

for tumor segmentation. In overcoming the limitations of existing methods, enhancement [132–134] and segmentation [135–137] have significance in tumor detection.

Feature extraction methods

The feature extraction approaches [12, 138–140] including GLCM [15, 141, 142], geometrical features (area, perimeter, and circularity) [15], first-order statistical (FOS), GWT [143, 144], Hu moment invariants (HMI) [145], multifractal features [146], 3D Haralick features [147], LBP [148], GWT [11], HOG [14, 137], texture and shape [82, 143, 149, 150], co-occurrence matrix, gradient, run-length matrix [151], SFTA, curvature features [152, 153], Gabor like multiscale texton features [154], Gabor wavelet and statistical features [142, 143] are utilized for classification. Table 3 lists the summary of feature extraction methods.

Feature selection methods or feature selection/reduction methods

In machine learning and computer vision applications, high-dimensional features maximize the system execution time and memory requirement for processing. Therefore, to distinguish between relevant and non-relevant features, several feature selection methods are required to minimize redundant information [168]. The optimal feature extraction is still a challenging task [47]. The single-point heuristic search method, ILS, genetic algorithm (GA) [169], GA+ fuzzy rough set [170], hybrid wrapper-filter [171], TRSFFQR, tolerance rough set (TRS), firefly algorithm (FA) [172], minimum redundancy maximum relevance (mRMR) [152], Kullback–Leibler divergence measure [173], iterative sparse representation [174], recursive feature elimination (RFE) [175], CSO-SIFT [176], entropy [11, 177, 178], PCA [179], and LDA [180] are utilized to remove redundant features. A summary of classification methods as shown in Table 4.

Classification methods

The classification approaches are used to categorize input data into different classes in which training and testing are performed on known and unknown samples [16, 24, 25, 181–192]. Machine learning is widely used for tumor classification into appropriate classes, e.g., tumor substructure (complete/non-enhanced/enhanced) [193], tumor and non-tumor [26], and benign and malignant tumor [15, 47, 163, 194, 195]. KNN [196], SVM, nearest subspace classifier, and representation classifier [143] are supervised, whereas FCM [197, 198], hidden Markova random field [199] self-organization map [101], and SSAE [200] are unsupervised methods.

Recent trends in medical imaging to detect malignancy

Deep learning and quantum machine learning methodologies are widely utilized for tumor localization and classification [201]. In these techniques, automatic feature learning helps to discriminate complicated patterns [186, 202–213].

Deep learning methods

The variety of state of the art deep learning methodologies are used to learn the data in the medical domain [214] including CNN [215, 216], Deep CNN, cascaded CNN [217], 3D-CNN [218], convolutional encoder network, LSTM, CRF [218], U-Net CNN [219], dual-force CNN [220] and WRN-PPNet [221].

The brain tumor classification problem has been solved by employing a LSTM model. In this method, input MRI images smooth using N4ITK and 5×5 Gaussian filter and passed as input to the four LSTM model. The LSTM model is constructed on the four hidden Units such as 200, 225, 200, 225, respectively. The performance of this model has been tested on BRATS (2012–2015 and 2018) series and SISS-2015

Table 3 Summary of the feature extraction methods

References	Year	Extracted features	Dataset	Results
[154]	2013	Gabor-like multiscale texton features	BRATS2012	0.73 DSC
[148]	2015	GLCM features	120 MR images	0.817 similarity index, 0.817 overlap function, 0.182 extra function, and 0.817 PPV
[15]	2017	Shape, texture, and intensity features	Harvard, RIDER, Private collected images	0.79 ACC on the cubic kernel of SVM (Private collected images), 0.96 ACC on the cubic kernel of SVM (RIDER), 0.87 ACC on the cubic kernel of SVM (Harvard)
[144]	2017	371 texture and intensity features	Harvard	0.9334 ACC
[145]	2017	Shape descriptor	90 MR images	0.9889 ACC
[146]	2017	Multi-fractal features	Harvard	98.01% ± 0.07 ACC, 1.00 SE, and 94.78% ± 0.02 SP
[147]	2017	GLCM, GLGCM, GLCCM and Tamura features	62 patients	0.7581 ACC, 0.8122 AUC
[14]	2018	GWF, HOG, LBP SFTA features	2012 Image, 2013 challenge, 2015 challenge [BRATS], ISLES 2015	0.98 SE on 2012 Image, 0.98 SE, on 2013 challenge, 0.98 SE, on 2015 challenge, 1.00 SE, on ISLES 2015
[11]	2019	LBP and GWF and fusion of both LBP and GWF features	BRATS2013 Challenge, BRATS 2015 Challenge Private collected images	1.00 SP on BRATS 2013, 0.90 SP on Fused feature vector (ensemble classifier) on BRATS 2015, 0.83 SP, 0.91 on Fused feature vector (ensemble classifier) on private collected images
[150]	2019	GLCM features	105 MR images	0.9882 ACC, 1.00 SE, 0.9783 SP, and 1.17 Error rate
[155]	2020	Stochastic texture features	9 Patients of BRATS 2015	0.852 ± 0.063 complete, 0.812 ± 0.074, 0.851 ± 0.093 enhance
[156]	2020	CNN, LBP, and HOG features	BRATS 2015	0.81 complete, 0.76 core and 0.73 enhance
[157]	2021	(PCA), entropy, mean, and wavelet transform	BRATS 2015	0.96 ACC

benchmark datasets [222]. In this work, a new framework is presented based on the fusion of different kinds of MRI sequences. The fused sequence provides more information as compared to single sequence. Later, fused sequence has been supplied to the 23 CNN model. The suggested model is trained on brat's series for the detection of glioma [16]. The 14 layers CNN model has been trained from the scratch on six Brats series datasets for detection of glioma and stroke lesions [25]. The classification is performed using ELM and RELM classifiers. This method has been tested on BRATS series such as 2012 to 2015 [189]. The 09-layer CNN model is trained from the scratch for classification of different types of tumors such as pituitary, glioma and meningioma. The method achieved an accuracy of the classification is 98.71% [223]. This model is trained from the scratch on publicly 696 weighted-T1 sequences. The model provides an accuracy of greater than 99% for tumor classification [224]. The existing methods are summarized in Table 5.

Although much work is done on deep learning methods, still there exist many challenges. The present methods do not

Table 4 Summary of the existing classification methods

References	Year	Methods	Classifiers	Datasets	MRI sequences	Classes	Results
[158]	2011	Wavelet transform, PCA, scaled conjugate gradient (SCG)	Neural network (NN)	Harvard	T2 weighted	Normal or abnormal	1.00 ACC
[159]	2012	PCC, PCA, and ICA	SVM	Private data	T2 weighted and T1 weighted	Low- and high-grade glioma	0.82 ACC at PCC, 0.85 ACC at PCA, 0.79 ACC at ICA
[160]	2013	Wavelet, shape, texture, and boundary features, ICA	Ensemble classifier (SVM,KNN, and ANN)	Private images collected from ShirdiSai Cancer Hospital	T1 weighted and T2 weighted	Benign and malignant	0.99 ACC, 1.00 SE, 0.98 SP
[45]	2014	Feedback PCNN (FPCNN), wavelet transform, PCA	ANN	14 normal and 87 abnormal images	T2 weighted	Normal and abnormal	0.99 ACC
[161]	2014	Multi-dimensional co-occurrence matrix	ELM-IPSO	35 clinical routine cases	T1 weighted and T1C weighted	Low and high-grade glioma	0.99 ACC, 0.95 SP and 0.98 SE
[162]	2015	N4ITK, histogram matching	Random decision forest (RDF)	BRATS 2013 Challenge	FLAIR, (T1T1C, and T2) weighted	Complete, core and enhance	0.86 complete.0.71 core,0.73 enhance DSC on LGG,0.76 complete,0.58 core, 0.16 enhance DSC on HGG
[163]	2015	Intensity, geometry, and asymmetry	RF	BRATS 2013 Challenge	FLAIR, T1, T1C, and T2 (weighted)	Complete, core and enhance	0.87 complete, 78 core, 74 enhance DSC, 85 complete,74 core, 69 enhance PPV, 89 complete,88 core, 83 enhance SE

Table 4 continued

References	Year	Methods	Classifiers	Datasets	MRI sequences	Classes	Results
[164]	2016	2D-DWT, Wavelet-energy	SVM	Harvard	T2 (weighted)	Normal and abnormal	0.97 ACC, 0.99 precision,0.92 SP, 0.98 SE
[82]	2017	Multi-level Otsu threshold, HOG-TOP	RF	BRATS 2013 synthetic	Flair	Complete, core and enhance	0.93 ± 0.04 HG DSC, 0.90 ± 0.02 LG DSC
[145]	2017	HMI	Twin SVM	Harvard	T2 weighted	Normal and abnormal	0.98 ACC, 0.99 SE, 0.92 SP
[146]	2017	Directional spectral distribution	SVM	Harvard	T2 weighted	Healthy and glioma	1.00 SE
[165]	2018	Stationary wavelet entropy (SWE)	Kernel support vector machine (KSVM)	Harvard	T2 weighted	Normal and abnormal	0.98 ACC, 0.99 precision, 0.96 SP, 0.98 SE
[166]	2018	Fractional Sobel filter, statistical features	SVM	BRATS 2013 challenge	T1 weighted and Flair	Tumor and healthy tissues	0.98 ACC, 0.86 SE, 0.98 SP
[27]	2020	Stacked sparse autoencoder (SSAE)	Softmax	2012, 2013, 2014, and 2015 BRATS	FLAIR, T1, T1C,T2 weighted	Normal and abnormal	100% on 2012, 90% on 2012 synthetic, 95% on 2013, 100% on Leaderboard 2013, 97% 2014 and 95%
[167]	2021	CNN	SVM	Local data	FLAIR, T1, T1C, T2 weighted	Grade I, II, III and IV	100%

Table 5 Summary of the deep learning methods

References	Year	DL model	Datasets (BRATS 2012–2019)	Types of tumor	Performance measures (DSC)		
					Complete	Core/non-enhanced	Enhanced
[225]	2014	CNN	2013	Glioma	83.7 ± 9.4	73.6 ± 25.6	69.0 ± 24.9
[226]	2015	CNN	2014		0.81 ± 15	0.79 ± 13	0.81 ± 11
[227]	2016	CNN	2013		0.88	0.83	0.77
[193]	2017	Input cascade CNN	2012		0.81	0.72	0.58
			2013 Leaderboard		0.84	0.71	0.57
			2013 Challenge		0.88	0.79	0.73
[219]	2017	U-Net CNN	2015		0.86	0.86	0.65
[218]	2017	DeepMedic + CRF	2015		0.84	0.67	0.62
			ISLES 2015		0.66 DSC	–	–
[228]	2018	FCNN + CRF	(2013 Challenge		0.85	0.83	0.74
			2013 Leaderboard		0.88	0.84	0.77
			2015 Challenge)		0.82	0.72	0.62
[229]	2018	DNN (ILinear nexus architecture)	2013		0.87	0.89	0.92
			2015		0.86	0.87	0.90
[220]	2019	Dual-force CNN	2015		0.83	0.67	0.63
			2017		0.87	0.73	0.69
[221]	2019	WRN-PPNet	2015		0.94	–	–
			2018		0.91		
[230]	2021	YOLOv2	2018, 2019, 2020		0.90	–	–
[231]	2020	3D U-Net and DeepMedic	2017		0.90	0.81	0.78
			2018				
[186]	2018	Patch-based CNN model	2015		0.95	–	–
			ISLES 2015	Stroke	1.00	–	–
			ISLES 2017		0.98	–	–
[217]	2016	CNN	ISLES 2015 (SISS, SPES)		0.59 on SISS, 0.77 on SPES	–	–

achieve maximum results in the sub-structure of the tumor region. For example, if the accuracy of the complete tumor is increased, then the accuracy of the core and the enhanced tumor is decreased (as shown in Table 5).

Brain tumor detection using transfer learning

The manual detection of brain tumors is difficult due to asymmetrical lesions shape, location flexibility, and unclear boundaries. Therefore, a transfer-learning model has been suggested based on the super-pixel. The VGG-19 is a pre-trained model that has been utilized for the classification of the different grades of the glioma such as high/low glioma. The method achieved 0.99 AUC on the brats 2019 series[232]. The three different types of pre-trained models i.e., VGG network, Google network and Alex network are employed on the brain datasets for the classification of glioma, pituitary and meningioma. In this method, augmentation methods are also employed on MRI slices to generalize the outcomes and reduced the overfitting problem by increasing the quantity of the input data. After the experimental analysis using different pre-trained models, we conclude that VGG-16 provides greater than 98% classification accuracy [233]. The classification of brain tumors has been done using two different types of networks, i.e., visual attention network and CNN are utilized for classification of different types of brain tumor i.e., glioma, pituitary I and meningioma [234]. A pre-trained model i.e., VGG-16, Alex and Google net are investigated for the analysis of brain tumors. The frequency domain techniques have been applied on input slices to improve the image contrast. The contrast improved images are passed in the next phase. Where pre-trained VGG-16 provides maximum classification outcomes [235]. The Laplacian filter with a multi-layered dictionary model is utilized for the recognition of brain tumors. The model performed better as compared to existing works [236]. The method consists of the three major steps such as pre-processing, augmentation of data, and segmentation and classification using transfer learning models. In which ResNet-50, DenseNet-201, MobileNet-v2 and Inceptionv3

Table 6 Summary of the transfer learning methods

References	Year	Methods	Datasets/images	Results
[241]	2019	Pre-trained Alex-net and Google net	BRATS [2013, 2014, 2015, 2016] and ISLES-2018	Up to 95% ACC
[16]	2020	Features from VGG-19 and LBP and HOG	BRATS) [2015, 2016, and 2017]	0.99, 1.00 and 0.99 Dice scores, respectively
[237]	2020	ResNet50, InceptionV3, MobileNet -V2, NASNet and DenseNet201	233 MRI patient's data	ACC of 92.9%, 92.8%, 91.8%, 99.6%, 93.1%, respectively
[235]	2020	Alexnet, Resnet50, GoogLeNet, VGG-16, Resnet101, VGG-19, Inceptionv3, and InceptionResNetV2	Harvard and local datasets	ACC of 100%, 94%, and 95.92%
[234]	2020	Pre-trained visual attention model	3064 tumor slices of local data	95.5% ACC
[233]	2020	Alex, Google and VGG	233 MRI patient's data	97.3% ACC
[232]	2020	VGG-19 with post-processing	2019 BRATS series	93.2 dice scores
[243]	2020	Inception-v3 and DensNet201	3064 tumor slices of local data	99.34%, and 99.51%
[244]	2020	ResNet-attention gate	BRATS (2017, 2018 and 2019)	86.5% ACC
[247]	2020	VGG19	233 MRI patient's data	96.13% ACC
[223]	2020	AlexNet, VGG16, ResNet18, ResNet50, VGG19, ResNet-Inception-v2, SENet, GoogleNet, ResNet101	233 MRI patient's data	Up to 95% ACC
[248]	2020	UNet-VGG16	Local data	Up to 96% ACC
[249]	2019	GoogLeNet	233 MRI patient's data	98% ACC
[250]	2019	AlexNet	Local data	100% ACC
[251]	2019	ResNet34	Local data	0.7380 ± 0.16 ACC
[252]	2020	InceptionV3	233 MRI patient's data	99% ACC
[253]	2020	InceptionV3, SqueezeNet, VGG19 and ResNet50	Local data	Up to 97% ACC
[254]	2018	AlexNet and GoogLeNet	Local data	Up to 80% ACC
[255]	2019	VGGNet and ResNet	Local data	97% ACC
[256]	2021	AlexNet	2019 BRATS	82% AUC
[257]	2021	Resnet-50, VGG-16 and Inception-V3	Local data	ACC of 95%, 90% and 55%, respectively
[240]	2021	ResNet, MobilNet-V2 and Xception	Local data	Up to 98% ACC
[239]	2021	ResNet-50 model with average global pooling	Local data	Up to 97% ACC
[238]	2021	8 layers of Alex-network	Local data	100% ACC

are utilized to classify the brain lesions with 0.95 IoU [237]. The deep features are extracted from the transfer learning AlexNet model. The model has eight layers, five of which are convolutional and three of which are fully linked. The SoftMax layer has been employed for classification between the different types of brain lesions [238]. The transfer learning ResNet-50 model with average global pooling is utilized to reduce the gradient vanishing and overfitting issues. The performance of this model has been evaluated on three distinct types of brain imaging benchmark samples that contain 3064 input images. The method achieved an accuracy of the 97.08% that is maximum as compared to latest existing works [239]. A deep CNN was used in this study that based on transfer learning such as ResNet, Xception and Mobilenetv2 are utilized for the extraction of deep features has been for tumors classification using MRI images. This method achieved an accuracy of up to 98% [240]. In this method, Grab Cut method has been employed for segmentation of the brain lesions. Later hand-crafted such as LBP features dimension of 1×20 and HOG features dimension of 1×100 are extracted and serially fused to the deep features dimension of 1×1000 that are extracted from the pre-trained VGG-19 model and final fused features vector length of $1 \times$ that is supplied to the different kind of classifiers. The experimental analysis proves that fused features vector provide good results as compared to existing work in this domain [16, 187]. The global thresholding method is applied to segment the actual lesion region. After segmentation, texture features such as LBP and GWF are extracted from the segmented images. After that, the retrieved features are fused to form a single fused feature vector, which is then provided to the classifiers for differentiation between healthy and unhealthy images [26]. There are two key stages to the procedure. The brain lesions are enhanced and segmented using spatial domain approaches in the first stage, then deep information's are extracted using pre-trained models, i.e., Alex and Google-network and score vector is achieved from softmax layer that is supplied to the classifiers such as for discrimination between the glioma/non-glioma images of brain. The Brats series dataset was used to test this technique's efficiency [241]. For brain tumor segmentation, the superpixel approach has been suggested. From the segmented images, Gabor wavelet information are retrieved and given to SVM and CRF for discrimination between the healthy/unhealthy MRI images [242].The transfer learning models such as inceptionv3, densenet-201, and to form a single vector, extracted features are merged serially and passed to softmax for tumor classification. Furthermore, different dense blocks of the densenet201 are extracted and classify the brain tumor using softmax. The approach had a 99% accuracy rate. The evaluation outcomes clearly state that the fused vector outperformed as compared to the single vector [243]. A novel U-net model with the RESnet model has been trained on the input MRI images. The classifiers are fed the salient features derived from its pictures. This method has been tested on BRATS 2017, 2018 and 2019 datasets [244]. The tumor region is localized on Flair sequences of brats 2012 series. The skull is removed from of the input pictures, and a noise-reduction filter is applied bilaterally. During the segmentation, texton features are recovered from the input images using the superpixel approach. For brain tumor classification, the leave out validation technique is used. This strategy yielded an 88 percent dice score [245]. The deep segmentation has been designed that contains two major parts such as encoder and decoder. The spatial information is extracted using a CNN in the encoder section. For determining the whole probability map resolution, the semantic mappings information is entered into the decoder component. On the basis of U-network distinct CNN networks such as ResNetwork, dense network and Nas-network are utilized for features extraction. This model has been tested successfully on Brats-2019 series. The method achieved dice scores of 0.84 [246]. The wavelet homomorphic filter has been employed for noise removal. The tumor infected region has been localized using improved YOLOv2 model [230]. The summary of the transfer learning methods is mentioned in Table 6.

Brain tumor detection using quantum machine learning

Superposition of quantum states/parallelism/entanglement can all be used to establish quantum computer supremacy [258]. However, exploring entanglement of quantum features for efficient computation is a difficult undertaking due to a shortage of computational resources for execution of quantum algorithms. With the progress of quantum techniques, classical computers based on quantum theory and influenced through qubits are no longer able to fully exploit the benefits of quantum state and entanglement. QANN has been found to be effective in a variety of computer tasks, including classification and pattern recognition due to the intrinsic properties supplied by quantum physics [259]. On the other hand, quantum models based on genuine quantum computers use big bits of the quantum/qubits as a simple representation of matrix and the linear functions. However, the computational complexity of the quantum-inspired neural network (QINN) designs increases several fold due to complicated and time-consuming back-propagation quantum model [260]. The automatic segmentation of brain lesions from I (MRI), which removes the onerous manual work of human specialists or radiologists, greatly aids brain tumor detection. Manually, brain tumor diagnosis, on the other hand, suffers from large variances in size, shape, orientation, illumination variations, greyish overlaying, and cross-heterogeneity. Scientists in the computer vision field have paid a lot of emphasis in recent

Table 7 Summary of the existing limitations of machine/deep learning methods

Ref	Year	Methods	Brain tumor types	Results	Problems/limitations
[267]	2015	Gaussian hidden markov random field (GHMRF)	Glioma (complete, core and enhance)	0.59 DSC on enhance tumor region	Enhance tumor region is not accurately/properly segmented using GHMRF
[145]	2017	Hu moment invariants (HMI) and SVM	Glioma/non-glioma	0.92 Specificity	The Hu moment invariants (HMI) with SVM cannot perform well on large scale dataset because SVM is employed for the recognition and SVM performs better on small scale datasets
[268]	2018	Gabor filter with RF	Glioma (complete, core and enhance)	0.84 DSC	Gabor filter with RF method fails in detecting tumor with small volume and its boundaries
[269]	2019	ALI, lesionGnb and LINDA methods	Stroke	0.50 Dice score (DC)	Due to variable size and stroke territory, ALI, lesionGnb and LINDA methods fail to detect the small lesion region
[220]	2019	DeepMedic and U-Net	Glioma (complete, core and enhance)	990.64 DSC	The enhance tumor region is segmented with less dice score compared to complete and non-enhance region
[266]	2020	Progressive growing of generative adversarial networks (GANs) (PGGANs)	Glioma/non-glioma	0.91 Accuracy	PGGANs method fails to differentiate tumor/non-tumor features in 25% cases
[270]	2020	Unsupervised probabilistic model	Glioma and stroke	0.34 ± 0.20 AUC	Fail to detect the small and unobvious brain lesions
[271]	2020	3D Squeeze-and-Excitation V-Net	Glioma (complete, core and enhance)	0.74 DSC enhance tumor,0.89 DSC complete tumor,0.80 DSC non-enhance	3D Squeeze-and-Excitation V-Net does not provide accurate tumor prediction in some cases
[272]	2021	Adaptive deep fuzzy neural model	Glioma/non- glioma	0.99 ACC	Computationally exhaustive still need to work on light weight model for accurate brain tumor detection

years to building robust and efficient automated segmentation approaches. The current research focuses on a unique quantum fully supervised learning process which is defined by qutrits for timely and effective lesions segmentation. The proposed work's main goal is to speed up the QFS-convergence Net's and make it appropriate for computerized segmentation of the brain lesions without the need for any learning/supervision. To leverage the properties of quantum correlation, suggested a quantum fully self-supervised neural network (QFS-Net) model uses qutrits/three states of quantum for segmentation of the brain lesions [261]. The QFS-Net uses a revolutionary fully supervised qutrit-based counter propagation method to replace the sophisticated quantum back-propagation method that utilized in supervised QINN networks. This approach allows for iterative quantum state that propagates among the layers of network.

Limitations of existing's machine/deep learning methods

In this survey, recent literature regarding the detection of brain tumors is reviewed, and it is indicated that there is still room for improvement. During image acquisition, noise is included in MRI, and noise removal is an intricate task [2, 262–264]. Accurate segmentation is a difficult task [265], as brain tumors have tentacles and diffused structures [43, 193, 220, 266]. Selecting and extracting optimal features and appropriate number of training/testing samples for better classification is also an important task [191, 192]. Deep learning models are gaining attention as the learning of features is accomplished automatically; however, they require high computing power and large memory. Therefore, still there is a need to design a lightweight model that provides high ACC in less computational time. Some existing machine learning methods with their limitations are mentioned in Table 7.

The following are the main challenges of brain tumor detection.

The glioma and stroke tumors are not well contrasted. It consists of tentacle and diffused structures that make segmentation and classification processes more challenging [270].

A small volume of tumor detection is still a challenge as it can be detected as a normal region [269, 273].

Some of the existing methods work well for only a complete tumor region and do not provide good results for other regions (enhanced, non-enhanced) and vice versa [267, 271, 274].

Research findings and discussion

After a comprehensive review of the state-of-the-art exiting methods, the following challenges are found:

- The size of a brain tumor grows rapidly. Therefore, tumor diagnosis at an initial stage is an exigent task.
- Brain tumor segmentation is difficult owing to the following factors.
- MRI image owing to magnetic field fluctuations in the coil.
- Gliomas are infiltrative, owing to fuzzy borders. Thus, they become more difficult to segment [43].
- Stroke lesion segmentation is a very intricate task, as stroke lesions appear in complex shapes and with ambiguous boundaries and intensity variations.
- The optimized and best feature extraction and selection is another difficult process inaccurate classification of brain tumors.

Conclusion

The accurate brain tumor detection is still very demanding because of tumor appearance, variable size, shape, and structure. Although tumor segmentation methods have shown high potential in analyzing and detecting the tumor in MR images, still many improvements are required to accurately segment and classify the tumor region. Existing work has limitations and challenges for identifying substructures of tumor region and classification of healthy and unhealthy images.

In short, this survey covers all important aspects and latest work done so far with their limitations and challenges. It will be helpful for the researchers to develop an understanding of doing new research in a short time and correct direction.

The deep learning methods have contributed significantly but still require a generic technique. These methods provided better results when training and testing are performed on similar acquisition characteristics (intensity range and resolution); however, a slight variation in the training and testing images directly affects the robustness of the methods. In future work, research can be conducted to detect brain tumors more accurately, using real patient data from any medium (different image acquisition (scanners). Handcrafted and deep features can be fused to improve the classification results. Similarly, lightweight methods such as quantum machine learning play significant role to improve the accuracy and efficacy that save the time of radiologists and increase the survival rate of patients.

Declarations

Conflict of interest There is no grant received from any resources. All authors declare that they have no conflict of interest.

Research involving human participants and/or animals It is declared that research has not involved any human participants and animals.

References

1. Park JG, Lee C (2009) Skull stripping based on region growing for magnetic resonance brain images. Neuroimage 47:1394–1407
2. Khan MA, Lali IU, Rehman A, Ishaq M, Sharif M, Saba T et al (2019) Brain tumor detection and classification: A framework of marker-based watershed algorithm and multilevel priority features selection. Microsc Res Tech 82:909–922
3. Raza M, Sharif M, Yasmin M, Masood S, Mohsin S (2012) Brain image representation and rendering: a survey. Res J Appl Sci Eng Technol 4:3274–3282
4. Watson C, Kirkcaldie M, Paxinos G (2010) The brain: an introduction to functional neuroanatomy. Academic Press, New York
5. (2015). https://en.wikipedia.org/wiki/Brain_size. Accessed 19 Oct 2019
6. Dubin MW (2013) How the brain works. Wiley, New York
7. Koziol LF, Budding DE, Chidekel D (2012) From movement to thought: executive function, embodied cognition, and the cerebellum. Cerebellum 11:505–525
8. Knierim J (1997) Neuroscience Online Chapter 5: Cerebellum. The University of Texas Health Science Center, Houston
9. Nuñez MA, Miranda JCF, de Oliveira E, Rubino PA, Voscoboinik S, Recalde R et al (2019) Brain stem anatomy and surgical approaches. Comprehensive overview of modern surgical approaches to intrinsic brain tumors. Elsevier, Amsterdam, pp 53–105
10. DeAngelis LM (2001) Brain tumors. N Engl J Med 344:114–123
11. Amin J, Sharif M, Raza M, Saba T, Sial R, Shad SA (2020) Brain tumor detection: a long short-term memory (LSTM)-based learning model. Neural Comput Appl 32:15965–15973
12. Sajjad S, Hanan Abdullah A, Sharif M, Mohsin S (2014) Psychotherapy through video game to target illness related problematic behaviors of children with brain tumor. Curr Med Imaging 10:62–72
13. Yasmin M, Sharif M, Masood S, Raza M, Mohsin S (2012) Brain image reconstruction: a short survey. World Appl Sci J 19:52–62
14. Amin J, Sharif M, Raza M, Yasmin M (2018) Detection of brain tumor based on features fusion and machine learning. J Ambient Intell Human Comput:1–17
15. Amin J, Sharif M, Yasmin M, Fernandes SL (2020) A distinctive approach in brain tumor detection and classification using MRI. Pattern Recogn Lett 139:118–127
16. Saba T, Mohamed AS, El-Affendi M, Amin J, Sharif M (2020) Brain tumor detection using fusion of hand crafted and deep learning features. Cogn Syst Res 59:221–230
17. Sharif M, Amin J, Nisar MW, Anjum MA, Muhammad N, Shad SA (2020) A unified patch based method for brain tumor detection using features fusion. Cogn Syst Res 59:273–286
18. Sharif M, Tanvir U, Munir EU, Khan MA, Yasmin M (2018) Brain tumor segmentation and classification by improved binomial thresholding and multi-features selection. J Ambient Intell Human Comput:1–20
19. Sharif MI, Li JP, Khan MA, Saleem MA (2020) Active deep neural network features selection for segmentation and recognition of brain tumors using MRI images. Pattern Recogn Lett 129:181–189
20. Sharif MI, Li JP, Naz J, Rashid I (2020) A comprehensive review on multi-organs tumor detection based on machine learning. Pattern Recogn Lett 131:30–37
21. Ohgaki H, Kleihues P (2013) The definition of primary and secondary glioblastoma. Clin Cancer Res 19:764–772
22. Cachia D, Kamiya-Matsuoka C, Mandel JJ, Olar A, Cykowski MD, Armstrong TS et al (2015) Primary and secondary gliosarcomas: clinical, molecular and survival characteristics. J Neurooncol 125:401–410
23. Amin J, Sharif M, Gul N, Yasmin M, Shad SA (2020) Brain tumor classification based on DWT fusion of MRI sequences using convolutional neural network. Pattern Recogn Lett 129:115–122
24. Sharif M, Amin J, Raza M, Yasmin M, Satapathy SC (2020) An integrated design of particle swarm optimization (PSO) with fusion of features for detection of brain tumor. Pattern Recogn Lett 129:150–157
25. Amin J, Sharif M, Anjum MA, Raza M, Bukhari SAC (2020) Convolutional neural network with batch normalization for glioma and stroke lesion detection using MRI. Cogn Syst Res 59:304–311
26. Amin J, Sharif M, Raza M, Saba T, Anjum MA (2019) Brain tumor detection using statistical and machine learning method. Comput Methods Progr Biomed 177:69–79
27. Amin J, Sharif M, Gul N, Raza M, Anjum MA, Nisar MW et al (2020) Brain tumor detection by using stacked autoencoders in deep learning. J Med Syst 44:32
28. Johnson DR, Guerin JB, Giannini C, Morris JM, Eckel LJ, Kaufmann TJ (2017) 2016 updates to the WHO brain tumor classification system: what the radiologist needs to know. Radiographics 37:2164–2180
29. Wright E, Amankwah EK, Winesett SP, Tuite GF, Jallo G, Carey C et al (2019) Incidentally found brain tumors in the pediatric population: a case series and proposed treatment algorithm. J Neurooncol 141:355–361
30. Pellegrino MP, Moreira F, Conforto AB (2021) Ischemic stroke. Neurocritical care for neurosurgeons. Springer, New York, pp 517–534
31. Garrick R, Rotundo E, Chugh SS, Brevik TA (2021) Acute kidney injury in the elderly surgical patient. Emergency general surgery in geriatrics. Springer, New York, pp 205–227
32. Lehmann ALCF, Alfieri DF, de Araújo MCM, Trevisani ER, Nagao MR, Pesente FS, Gelinski JR, de Freitas LB, Flauzino T, Lehmann MF, Lozovoy MAB (2021) Carotid intima media thickness measurements coupled with stroke severity strongly predict short-term outcome in patients with acute ischemic stroke: a machine learning study. Metab Brain Dis 36:1747–1761
33. Scott AM (2005) PET imaging in oncology. In: Bailey DL, Townsend DW, Valk PE, Maisey MN (eds) Positron emission tomography. Springer, London, pp 311–325
34. Wong TZ, van der Westhuizen GJ, Coleman RE (2002) Positron emission tomography imaging of brain tumors. Neuroimaging Clin 12:615–626
35. Wong KP, Feng D, Meikle SR, Fulham MJ (2002) Segmentation of dynamic PET images using cluster analysis. IEEE Trans Nuclear Sci 49:200–207
36. Brenner DJ, Hall EJ (2007) Computed tomography—an increasing source of radiation exposure. N Engl J Med 357:2277–2284
37. Smith-Bindman R, Lipson J, Marcus R, Kim K-P, Mahesh M, Gould R et al (2009) Radiation dose associated with common computed tomography examinations and the associated lifetime attributable risk of cancer. Arch Intern Med 169:2078–2086

38. Fink JR, Muzi M, Peck M, Krohn KA (2015) Multimodality brain tumor imaging: MR imaging, PET, and PET/MR imaging. J Nucl Med 56:1554–1561
39. Hess CP, Purcell D (2012) Exploring the brain: Is CT or MRI better for brain imaging. UCSF Dep Radiol Biomed Imaging 11:1–11
40. Saad NM, Bakar SARSA, Muda AS, Mokji MM (2015) Review of brain lesion detection and classification using neuroimaging analysis techniques. J Teknol 74:1–13
41. Huang M, Yang W, Wu Y, Jiang J, Chen W, Feng Q (2014) Brain tumor segmentation based on local independent projection-based classification. IEEE Trans Biomed Eng 61:2633–2645
42. Khan MA, Arshad H, Nisar W, Javed MY, Sharif M (2021) An integrated design of Fuzzy C-means and NCA-based multi-properties feature reduction for brain tumor recognition. Signal and image processing techniques for the development of intelligent healthcare systems. Springer, New York, pp 1–28
43. Rewari R (2021) Automatic tumor segmentation from MRI scans. Stanford University, Stanford
44. Tandel GS, Biswas M, Kakde OG, Tiwari A, Suri HS, Turk M et al (2019) a review on a deep learning perspective in brain cancer classification. Cancers 11:1–32
45. El-Dahshan E-SA, Mohsen HM, Revett K, Salem A-BM (2014) Computer-aided diagnosis of human brain tumor through MRI: A survey and a new algorithm. Expert Syst Appl 41:5526–5545
46. Gordillo N, Montseny E, Sobrevilla P (2013) State of the art survey on MRI brain tumor segmentation. Magn Reson Imaging 31:1426–1438
47. Mohan G, Subashini MM (2018) MRI based medical image analysis: Survey on brain tumor grade classification. Biomed Signal Process Control 39:139–161
48. Amin J, Sharif M, Yasmin M (2016) Segmentation and classification of lung cancer: a review. Immunol Endocr Metab Agents Med Chem 16:82–99
49. Shahzad A, Sharif M, Raza M, Hussain K (2008) Enhanced watershed image processing segmentation. J Inf Commun Technol 2:9
50. Joo L, Jung SC, Lee H, Park SY, Kim M, Park JE et al (2021) Stability of MRI radiomic features according to various imaging parameters in fast scanned T2-FLAIR for acute ischemic stroke patients. Sci Rep 11:1–11
51. Chen H, Zou Q, Wang Q (2021) Clinical manifestations of ultrasonic virtual reality in the diagnosis and treatment of cardiovascular diseases. J Healthc Eng 2021:1–12
52. Henneghan AM, Van Dyk K, Kaufmann T, Harrison R, Gibbons C, Heijnen C, Kesler SR (2021) Measuring self-reported cancer-related cognitive impairment: recommendations from the Cancer Neuroscience Initiative Working Group. JNCI:1–9
53. Drake-Pérez M, Boto J, Fitsiori A, Lovblad K, Vargas MI (2018) Clinical applications of diffusion weighted imaging in neuroradiology. Insights Imaging 9:535–547
54. Okorie CK, Ogbole GI, Owolabi MO, Ogun O, Adeyinka A, Ogunniyi A (2015) Role of diffusion-weighted imaging in acute stroke management using low-field magnetic resonance imaging in resource-limited settings. West Afr J Radiol 22:61
55. Menze BH, Jakab A, Bauer S, Kalpathy-Cramer J, Farahani K, Kirby J et al (2014) The multimodal brain tumor image segmentation benchmark (BRATS). IEEE Trans Med Imaging 34:1993–2024
56. Bakas S, Akbari H, Sotiras A, Bilello M, Rozycki M, Kirby JS et al (2017) Advancing the cancer genome atlas glioma MRI collections with expert segmentation labels and radiomic features. Sci Data 4:170117
57. Kistler M, Bonaretti S, Pfahrer M, Niklaus R, Büchler P (2013) The virtual skeleton database: an open access repository for biomedical research and collaboration. J Med Internet Res 15:e245
58. Summers D (2003) Harvard whole brain Atlas: www. med. harvard. edu/AANLIB/home. html. J Neurol Neurosurg Psychiatry 74:288–288
59. Armato S, Beichel R, Bidaut L, Clarke L, Croft B, Fenimore C, Gavrielides M et al (2008) RIDER (Reference Database to Evaluate Response) Committee Combined Report, 9/25/2008 Sponsored by NIH, NCI, CIP, ITDB Causes of and Methods for Estimating/Ameliorating variance in the evaluation of tumor change in response-to therapy. https://wiki.cancerimagingarchive.net/display/Public/Collections
60. Kistler M, Bonaretti S, Pfahrer M, Niklaus R, Büchler P (2013) The virtual skeleton database: an open access repository for biomedical research and collaboration. J Med Internet Res 15:1–14
61. Yasmin M, Mohsin S, Sharif M, Raza M, Masood S (2012) Brain image analysis: a survey. World Appl Sci J 19:1484–1494
62. Somasundaram K, Kalaiselvi T (2010) Fully automatic brain extraction algorithm for axial T2-weighted magnetic resonance images. Comput Biol Med 40:811–822
63. Zhu Y, Young GS, Xue Z, Huang RY, You H, Setayesh K et al (2012) Semi-automatic segmentation software for quantitative clinical brain glioblastoma evaluation. Acad Radiol 19:977–985
64. Prabhu LAJ, Jayachandran A (2018) Mixture model segmentation system for parasagittal meningioma brain tumor classification based on hybrid feature vector. J Med Syst 42:1–6
65. Park CR, Kim K, Lee Y (2019) Development of a bias field-based uniformity correction in magnetic resonance imaging with various standard pulse sequences. Optik 178:161–166
66. Patel P, Bhandari A (2019) A review on image contrast enhancement techniques. Int J Online Sci 5:14–18
67. Zhang Z, Song J (2019) A robust brain MRI segmentation and bias field correction method integrating local contextual information into a clustering model. Appl Sci 9:1332
68. Irum I, Sharif M, Yasmin M, Raza M, Azam F (2014) A noise adaptive approach to impulse noise detection and reduction. Nepal J Sci Technol 15:67–76
69. Robb RA (2000) 3-dimensional visualization in medicine and biology. Handb Med Imaging Process Anal:685–712
70. Mehmood I, Ejaz N, Sajjad M, Baik SW (2013) Prioritization of brain MRI volumes using medical image perception model and tumor region segmentation. Comput Biol Med 43:1471–1483
71. Lu X, Huang Z, Yuan Y (2015) MR image super-resolution via manifold regularized sparse learning. Neurocomputing 162:96–104
72. Irum I, Sharif M, Raza M, Mohsin S (2015) A nonlinear hybrid filter for salt & pepper noise removal from color images. J Appl Res Technol 13:79–85
73. Stadler A, Schima W, Ba-Ssalamah A, Kettenbach J, Eisenhuber E (2007) Artifacts in body MR imaging: their appearance and how to eliminate them. Eur Radiol 17:1242–1255
74. Masood S, Sharif M, Masood A, Yasmin M, Raza M (2015) A survey on medical image segmentation. Curr Med Imaging 11:3–14
75. Irum I, Sharif M, Raza M, Yasmin M (2014) Salt and pepper noise removal filter for 8-bit images based on local and global occurrences of grey levels as selection indicator. Nepal J Sci Technol 15:123–132
76. Sharif M, Irum I, Yasmin M, Raza M (2017) Salt & pepper noise removal from digital color images based on mathematical morphology and fuzzy decision. Nepal J Sci Technol 18:1–7
77. Prastawa M, Bullitt E, Moon N, Van Leemput K, Gerig G (2003) Automatic brain tumor segmentation by subject specific modification of atlas priors1. Acad Radiol 10:1341–1348
78. Wu Y, Yang W, Jiang J, Li S, Feng Q, Chen W (2013) Semi-automatic segmentation of brain tumors using population and individual information. J Digit Imaging 26:786–796

79. Xie K, Yang J, Zhang Z, Zhu Y (2005) Semi-automated brain tumor and edema segmentation using MRI. Eur J Radiol 56:12–19
80. Agn M, Puonti O, af Rosenschöld PM, Law I, Van Leemput K (2015) Brain tumor segmentation using a generative model with an RBM prior on tumor shape. In: BrainLes vol 2015, pp 168–180
81. Haeck T, Maes F, Suetens P (2015) ISLES challenge 2015: Automated model-based segmentation of ischemic stroke in MR images. BrainLes 2015:246–253
82. Abbasi S, Tajeripour F (2017) Detection of brain tumor in 3D MRI images using local binary patterns and histogram orientation gradient. Neurocomputing 219:526–535
83. Sauwen N, Acou M, Sima DM, Veraart J, Maes F, Himmelreich U et al (2017) Semi-automated brain tumor segmentation on multi-parametric MRI using regularized non-negative matrix factorization. BMC Med Imaging 17:29
84. Ilunga-Mbuyamba E, Avina–Cervantes JG, Garcia-Perez A, de Jesus Romero–Troncoso R, Aguirre–Ramos H, Cruz–Aceves I et al (2017) Localized active contour model with background intensity compensation applied on automatic MR brain tumor segmentation. Neurocomputing 220:84–97
85. Akbar S, Akram MU, Sharif M, Tariq A, Khan SA (2018) Decision support system for detection of hypertensive retinopathy using arteriovenous ratio. Artif Intell Med 90:15–24
86. Banerjee S, Mitra S, Shankar BU (2018) Automated 3D segmentation of brain tumor using visual saliency. Inf Sci 424:337–353
87. Raja NSM, Fernandes SL, Dey N, Satapathy SC, Rajinikanth V (2018) Contrast enhanced medical MRI evaluation using Tsallis entropy and region growing segmentation. J Ambient Intell Human Comput:1–12
88. Subudhi A, Dash M, Sabut S (2020) Automated segmentation and classification of brain stroke using expectation-maximization and random forest classifier. Biocybern Biomed Eng 40:277–289
89. Gupta N, Bhatele P, Khanna P (2019) Glioma detection on brain MRIs using texture and morphological features with ensemble learning. Biomed Signal Process Control 47:115–125
90. Myronenko A, Hatamizadeh A (2020) Robust semantic segmentation of brain tumor regions from 3D MRIs. arXiv:2001.02040
91. Karayegen G, Aksahin MF (2021) Brain tumor prediction on MR images with semantic segmentation by using deep learning network and 3D imaging of tumor region. Biomed Signal Process Control 66:102458
92. Prima S, Ayache N, Barrick T, Roberts N (2001) Maximum likelihood estimation of the bias field in MR brain images: Investigating different modelings of the imaging process. In: International conference on medical image computing and computer-assisted intervention, pp 811–819
93. Haider W, Sharif M, Raza M (2011) Achieving accuracy in early stage tumor identification systems based on image segmentation and 3D structure analysis. Comput Eng Intell Syst 2:96–102
94. Irum I, Shahid MA, Sharif M, Raza M (2015) A review of image denoising methods. J Eng Sci Technol Rev 8:1–11
95. Kumar SS, Dharun VS (2016) A study of MRI segmentation methods in automatic brain tumor detection. Int J Eng Technol 8:609–614
96. Dhas A, Madheswaran M (2018) An improved classification system for brain tumours using wavelet transform and neural network. West Indian Med J 67:243–247
97. Krissian K, Aja-Fernández S (2009) Noise-driven anisotropic diffusion filtering of MRI. IEEE Trans Image Process 18:2265–2274
98. Tahir B, Iqbal S, Usman Ghani Khan M, Saba T, Mehmood Z, Anjum A et al (2019) Feature enhancement framework for brain tumor segmentation and classification. Microsc Res Tech 82:803–811
99. Said AB, Hadjidj R, Foufou S (2019) Total variation for image denoising based on a novel smart edge detector: an application to medical images. J Math Imaging Vision 61:106–121
100. Bojorquez JAZ, Jodoin P-M, Bricq S, Walker PM, Brunotte F, Lalande A (2019) Automatic classification of tissues on pelvic MRI based on relaxation times and support vector machine. PLoS ONE 14:1–17
101. Sandhya G, Kande GB, Satya ST (2019) An efficient MRI brain tumor segmentation by the fusion of active contour model and self-organizing-map. J Biomim Biomater Biomed Eng 40:79–91
102. Yang Y, Huang S (2006) Novel statistical approach for segmentation of brain magnetic resonance imaging using an improved expectation maximization algorithm. Opt Appl 36:125–136
103. Mittal M, Goyal LM, Kaur S, Kaur I, Verma A, Hemanth DJ (2019) Deep learning based enhanced tumor segmentation approach for MR brain images. Appl Soft Comput 78:346–354
104. Roy S, Bandyopadhyay SK (2012) Detection and quantification of brain tumor from MRI of brain and it's symmetric analysis. Int J Inf Commun Technol Res 2:1–7
105. Gao J, Xie M (2009) Skull-stripping MR brain images using anisotropic diffusion filtering and morphological processing. In: 2009 IEEE international symposium on computer network and multimedia technology, pp 1–4
106. Maintz JA, Viergever MA (1998) A survey of medical image registration. Med Image Anal 2:1–36
107. Sharma P, Diwakar M, Choudhary S (2012) Application of edge detection for brain tumor detection. Int J Comput Appl 58:1–6
108. Popescu V, Battaglini M, Hoogstrate W, Verfaillie SC, Sluimer I, van Schijndel RA et al (2012) Optimizing parameter choice for FSL-brain extraction tool (BET) on 3D T1 images in multiple sclerosis. Neuroimage 61:1484–1494
109. Despotović I, Goossens B, Philips W (2015) MRI segmentation of the human brain: challenges, methods, and applications. Comput Math Methods Med 2015:1–23
110. Wong KP (2005) Medical image segmentation: methods and applications in functional imaging. In: Handbook of biomedical image analysis, pp 111–182
111. Chae SY, Suh S, Ryoo I, Park A, Noh KJ, Shim H et al (2017) A semi-automated volumetric software for segmentation and perfusion parameter quantification of brain tumors using 320-row multidetector computed tomography: a validation study. Neuroradiology 59:461–469
112. Sauwen N, Acou M, Sima DM, Veraart J, Maes F, Himmelreich U et al (2017) Semi-automated brain tumor segmentation on multi-parametric MRI using regularized non-negative matrix factorization. BMC Med Imaging 17:1–14
113. Foo JL (2006) A survey of user interaction and automation in medical image segmentation methods. In: Tech rep ISUHCI20062, Human Computer Interaction Department, Iowa State Univ, pp 1–11
114. Işın A, Direkoğlu C, Şah M (2016) Review of MRI-based brain tumor image segmentation using deep learning methods. Procedia Comput Sci 102:317–324
115. Shanthi KJ, Kumar MS (2007) Skull stripping and automatic segmentation of brain MRI using seed growth and threshold techniques. In: 2007 International conference on intelligent and advanced systems, pp 422–426
116. Yao J (2006) Image processing in tumor imaging, new techniques in oncologic imaging. Zhang, F., & Hancock, ER Zhang. New Riemannian techniques for directional and tensorial image data. Pattern Recogn 43:1590–1606
117. Stadlbauer A, Moser E, Gruber S, Buslei R, Nimsky C, Fahlbusch R et al (2004) Improved delineation of brain tumors: an automated method for segmentation based on pathologic changes of 1H-MRSI metabolites in gliomas. Neuroimage 23:454–461
118. Lakare S, Kaufman A (2000) 3D segmentation techniques for medical volumes, Center for Visual Computing. Department of Computer Science, State University of New York, New York, pp 59–68

119. Sato M, Lakare S, Wan M, Kaufman A, Nakajima M (2000) A gradient magnitude based region growing algorithm for accurate segmentation. In: Proceedings 2000 International Conference on Image Processing, vol 3, pp 448–451
120. Salman YM (2009) Modified technique for volumetric brain tumor measurements. J Biomed Sci Eng 2:16
121. Singh NP, Dixit S, Akshaya AS, Khodanpur BI (2017) Gradient magnitude based watershed segmentation for brain tumor segmentation and classification. In: Proceedings of the 5th international conference on frontiers in intelligent computing: theory and applications, pp 611–619
122. Husain RA, Zayed AS, Ahmed WM, Elhaji HS (2015) Image segmentation with improved watershed algorithm using radial bases function neural networks. In: 2015 16th International conference on sciences and techniques of automatic control and computer engineering (STA), pp 121–126
123. Masood S, Sharif M, Yasmin M, Raza M, Mohsin S (2013) Brain image compression: a brief survey. Res J Appl Sci Eng Technol 5:49–59
124. Mughal B, Muhammad N, Sharif M (2018) Deviation analysis for texture segmentation of breast lesions in mammographic images. Eur Phys J Plus 133:1–15
125. Anjum MA, Amin J, Sharif M, Khan HU, Malik MSA, Kadry S (2020) Deep semantic segmentation and multi-class skin lesion classification based on convolutional neural network. IEEE Access 8:129668–129678
126. Gies V, Bernard TM (2004) Statistical solution to watershed over-segmentation. In: 2004 International Conference on Image Processing. ICIP'04, vol 3, pp 1863–1866
127. Kong J, Wang J, Lu Y, Zhang J, Li Y, Zhang B (2006) A novel approach for segmentation of MRI brain images. In: MELECON 2006-2006 IEEE Mediterranean Electrotechnical Conference, pp 525–528
128. Couprie M, Bertrand G (1997) Topological gray-scale watershed transformation. In: Vision Geometry VI International Society for Optics and Photonics, vol 3168, pp 136–146
129. Lotufo RA, Falcão AX, Zampirolli FA (2002) IFT-watershed from gray-scale marker. In: Proceedings. XV Brazilian Symposium on Computer Graphics and Image Processing, pp 146–152
130. Benson CC, Lajish VL, Rajamani K (2015) Brain tumor extraction from MRI brain images using marker based watershed algorithm. In: 2015 International Conference on advances in computing, communications and informatics (ICACCI), pp 318–323
131. Nasir M, Attique Khan M, Sharif M, Lali IU, Saba T, Iqbal T (2018) An improved strategy for skin lesion detection and classification using uniform segmentation and feature selection based approach. Microsc Res Tech 81:528–543
132. Yasmin M, Sharif M, Masood S, Raza M, Mohsin S (2012) Brain image enhancement—a survey. World Appl Sci J 17:1192–1204
133. Shah GA, Khan A, Shah AA, Raza M, Sharif M (2015) A review on image contrast enhancement techniques using histogram equalization. Sci Int 27:1-10
134. Khan MA, Akram T, Sharif M, Shahzad A, Aurangzeb K, Alhussein M et al (2018) An implementation of normal distribution based segmentation and entropy controlled features selection for skin lesion detection and classification. BMC Cancer 18:1–20
135. Khan MA, Akram T, Sharif M, Saba T, Javed K, Lali IU et al (2019) Construction of saliency map and hybrid set of features for efficient segmentation and classification of skin lesion. Microsc Res Tech 82:741–763
136. Akram T, Khan MA, Sharif M, Yasmin M (2018) Skin lesion segmentation and recognition using multichannel saliency estimation and M-SVM on selected serially fused features. J Ambient Intell Human Comput:1–20
137. Yasmin M, Sharif M, Mohsin S, Azam F (2014) Pathological brain image segmentation and classification: a survey. Curr Med Imaging 10:163–177
138. Mughal B, Muhammad N, Sharif M (2018) Deviation analysis for texture segmentation of breast lesions in mammographic images. Eur Phys J Plus 133:455
139. Hameed M, Sharif M, Raza M, Haider SW, Iqbal M (2012) Framework for the comparison of classifiers for medical image segmentation with transform and moment based features. Res J Recent Sci 2277:2502
140. Irum I, Raza M, Sharif M (2012) Morphological techniques for medical images: a review. Res J Appl Sci Eng Technol 4:2948–2962
141. Jafarpour S, Sedghi Z, Amirani MC (2012) A robust brain MRI classification with GLCM features. Int J Comput Appl 37:1–5
142. Mughal B, Muhammad N, Sharif M (2019) Adaptive hysteresis thresholding segmentation technique for localizing the breast masses in the curve stitching domain. Int J Med Inf 126:26–34
143. Nabizadeh N, Kubat M (2015) Brain tumors detection and segmentation in MR images: Gabor wavelet vs. statistical features. Comput Electr Eng 45:286–301
144. Tiwari P, Sachdeva J, Ahuja CK, Khandelwal N (2017) Computer aided diagnosis system—a decision support system for clinical diagnosis of brain tumours. Int J Comput Intell Syst 10:104–119
145. Zhang Y, Yang J, Wang S, Dong Z, Phillips P (2017) Pathological brain detection in MRI scanning via Hu moment invariants and machine learning. J Exp Theor Artif Intell 29:299–312
146. Lahmiri S (2017) Glioma detection based on multi-fractal features of segmented brain MRI by particle swarm optimization techniques. Biomed Signal Process Control 31:148–155
147. Xu X, Zhang X, Tian Q, Zhang G, Liu Y, Cui G et al (2017) Three-dimensional texture features from intensity and high-order derivative maps for the discrimination between bladder tumors and wall tissues via MRI. Int J Comput Assist Radiol Surg 12:645–656
148. Shanthakumar P, Ganeshkumar P (2015) Performance analysis of classifier for brain tumor detection and diagnosis. Comput Electr Eng 45:302–311
149. Zhang B, Chang K, Ramkissoon S, Tanguturi S, Bi WL, Reardon DA et al (2017) Multimodal MRI features predict isocitrate dehydrogenase genotype in high-grade gliomas. Neuro Oncol 19:109–117
150. Srinivas B, Rao GS (2019) Performance evaluation of fuzzy C means segmentation and support vector machine classification for MRI brain tumor. In: Soft computing for problem solving. Springer, New York, pp 355–367
151. Herlidou-Meme S, Constans J, Carsin B, Olivie D, Eliat P, Nadal-Desbarats L et al (2003) MRI texture analysis on texture test objects, normal brain and intracranial tumors. Magn Reson Imaging 21:989–993
152. Soltaninejad M, Yang G, Lambrou T, Allinson N, Jones TL, Barrick TR et al (2017) Automated brain tumour detection and segmentation using superpixel-based extremely randomized trees in FLAIR MRI. Int J Comput Assist Radiol Surg 12:183–203
153. Yang D, Rao G, Martinez J, Veeraraghavan A, Rao A (2015) Evaluation of tumor-derived MRI-texture features for discrimination of molecular subtypes and prediction of 12-month survival status in glioblastoma. Med Phys 42:6725–6735
154. Islam A, Reza SM, Iftekharuddin KM (2013) Multifractal texture estimation for detection and segmentation of brain tumors. IEEE Trans Biomed Eng 60:3204–3215
155. Pei L, Bakas S, Vossough A, Reza SM, Davatzikos C, Iftekharuddin KM (2020) Longitudinal brain tumor segmentation prediction in MRI using feature and label fusion. Biomed Signal Process Control 55:101648

156. Khan H, Shah PM, Shah MA, ul Islam S, Rodrigues JJ (2020) Cascading handcrafted features and convolutional neural network for IoT-enabled brain tumor segmentation. Comput Commun 153:196–207
157. Dixit A, Nanda A (2021) An improved whale optimization algorithm-based radial neural network for multi-grade brain tumor classification. Visual Comput:1–16
158. Zhang Y, Dong Z, Wu L, Wang S (2011) A hybrid method for MRI brain image classification. Expert Syst Appl 38:10049–10053
159. Zöllner FG, Emblem KE, Schad LR (2012) SVM-based glioma grading: optimization by feature reduction analysis. Z Med Phys 22:205–214
160. Arakeri MP, Reddy GRM (2015) Computer-aided diagnosis system for tissue characterization of brain tumor on magnetic resonance images. SIViP 9:409–425
161. Nachimuthu DS, Baladhandapani A (2014) Multidimensional texture characterization: on analysis for brain tumor tissues using MRS and MRI. J Digit Imaging 27:496–506
162. Pinto A, Pereira S, Dinis H, Silva CA, Rasteiro DM (2015) Random decision forests for automatic brain tumor segmentation on multi-modal MRI images. In: 2015 IEEE 4th Portuguese meeting on bioengineering (ENBENG), pp 1–5
163. Tustison NJ, Shrinidhi K, Wintermark M, Durst CR, Kandel BM, Gee JC et al (2015) Optimal symmetric multimodal templates and concatenated random forests for supervised brain tumor segmentation (simplified) with ANTsR. Neuroinformatics 13:209–225
164. Yang G, Zhang Y, Yang J, Ji G, Dong Z, Wang S et al (2016) Automated classification of brain images using wavelet-energy and biogeography-based optimization. Multimedia Tools Appl 75:15601–15617
165. Wang S, Du S, Atangana A, Liu A, Lu Z (2018) Application of stationary wavelet entropy in pathological brain detection. Multimedia Tools Appl 77:3701–3714
166. Padlia M, Sharma J (2019) Fractional Sobel filter based brain tumor detection and segmentation using statistical features and SVM. In: Nanoelectronics, circuits and communication systems, pp 161–175
167. Ayadi W, Elhamzi W, Charfi I, Atri M (2021) Deep CNN for brain tumor classification. Neural Process Lett 53:671–700
168. Afza F, Khan MA, Sharif M, Rehman A (2019) Microscopic skin laceration segmentation and classification: a framework of statistical normal distribution and optimal feature selection. Microsc Res Tech 82:1471–1488
169. Adair J, Brownlee A, Ochoa G (2017) Evolutionary algorithms with linkage information for feature selection in brain computer interfaces. In: Advances in computational intelligence systems. Springer, New York, pp 287–307
170. Sharma M, Mukharjee S (2012) Brain tumor segmentation using hybrid genetic algorithm and artificial neural network fuzzy inference system (anfis). Int J Fuzzy Logic Syst 2:31–42
171. Huda S, Yearwood J, Jelinek HF, Hassan MM, Fortino G, Buckland M (2016) A hybrid feature selection with ensemble classification for imbalanced healthcare data: a case study for brain tumor diagnosis. IEEE Access 4:9145–9154
172. Jothi G (2016) Hybrid tolerance rough set-firefly based supervised feature selection for MRI brain tumor image classification. Appl Soft Comput 46:639–651
173. Ahmed S, Iftekharuddin KM, Vossough A (2011) Efficacy of texture, shape, and intensity feature fusion for posterior-fossa tumor segmentation in MRI. IEEE Trans Inf Technol Biomed 15:206–213
174. Wu G, Chen Y, Wang Y, Yu J, Lv X, Ju X et al (2018) Sparse representation-based Radiomics for the diagnosis of brain tumors. IEEE Trans Med Imaging 37:893–905
175. Fernandez-Lozano C, Seoane JA, Gestal M, Gaunt TR, Dorado J, Campbell C (2015) Texture classification using feature selection and kernel-based techniques. Soft Comput 19:2469–2480
176. Dandu JR, Thiyagarajan AP, Murugan PR, Govindaraj V (2019) Brain and pancreatic tumor segmentation using SRM and BPNN classification. Health Technol:1–9
177. Saritha M, Joseph KP, Mathew AT (2013) Classification of MRI brain images using combined wavelet entropy based spider web plots and probabilistic neural network. Pattern Recogn Lett 34:2151–2156
178. Sharif M, Khan MA, Akram T, Javed MY, Saba T, Rehman A (2017) A framework of human detection and action recognition based on uniform segmentation and combination of Euclidean distance and joint entropy-based features selection. EURASIP J Image Video Process 2017:1–18
179. Lakshmi A, Arivoli T, Rajasekaran MP (2018) A Novel M-ACA-based tumor segmentation and DAPP feature extraction with PPCSO-PKC-based MRI classification. Arab J Sci Eng 43:7095–7111
180. Rathi V, Palani S (2012) Brain tumor MRI image classification with feature selection and extraction using linear discriminant analysis. arXiv:1208.2128
181. Naqi SM, Sharif M, Yasmin M (2018) Multistage segmentation model and SVM-ensemble for precise lung nodule detection. Int J Comput Assist Radiol Surg 13:1083–1095
182. Amin J, Anjum MA, Sharif M, Kadry S, Nam Y, Wang S (2021) Convolutional bi-LSTM based human gait recognition using video sequences. CMC Comput Mater Contin 68:2693–2709
183. Amin J, Sharif M, Anjum MA, Nam Y, Kadry S, Taniar D (2021) Diagnosis of COVID-19 infection using three-dimensional semantic segmentation and classification of computed tomography images. Comput Mater Contin:2451–2467
184. Amin J, Sharif M, Raza M, Saba T, Rehman A (2019) Brain tumor classification: feature fusion. In: 2019 international conference on computer and information sciences (ICCIS), pp 1–6
185. Amin J, Sharif M, Yasmin M, Ali H, Fernandes SL (2017) A method for the detection and classification of diabetic retinopathy using structural predictors of bright lesions. J Comput Sci 19:153–164
186. Amin J, Sharif M, Yasmin M, Fernandes SL (2018) Big data analysis for brain tumor detection: deep convolutional neural networks. Futur Gener Comput Syst 87:290–297
187. Amin J, Sharif M, Yasmin M, Fernandes SL (2020) A distinctive approach in brain tumor detection and classification using MRI. Pattern Recogn Lett 139:118–127
188. Muhammad N, Sharif M, Amin J, Mehboob R, Gilani SA, Bibi N et al (2018) Neurochemical alterations in sudden unexplained perinatal deaths—a review. Front Pediatr 6:6
189. Sharif M, Amin J, Raza M, Anjum MA, Afzal H, Shad SA (2020) Brain tumor detection based on extreme learning. Neural Comput Appl:1–13
190. Umer MJ, Amin J, Sharif M, Anjum MA, Azam F, Shah JH (2021) An integrated framework for COVID-19 classification based on classical and quantum transfer learning from a chest radiograph. Concurr Comput Pract Exp 19:153–164
191. Jiang J, Wu Y, Huang M, Yang W, Chen W, Feng Q (2013) Brain tumor segmentation in multimodal MR images based on learning population-and patient-specific feature sets. Comput Med Imaging Graph 37:512–521
192. Ortiz A, Gorriz JM, Ramírez J, Salas-Gonzalez D, Alzheimer's Disease Neuroimaging Initiative (2013) Improving MRI segmentation with probabilistic GHSOM and multiobjective optimization 114:118–131
193. Havaei M, Davy A, Warde-Farley D, Biard A, Courville A, Bengio Y, Pal C, Jodoin PM, Larochelle H (2017) Brain tumor segmentation with deep neural networks. Med Image Anal 35:18–31

194. Zhang N, Ruan S, Lebonvallet S, Liao Q, Zhu Y (2011) Kernel feature selection to fuse multi-spectral MRI images for brain tumor segmentation. Comput Vis Image Underst 115:256–269
195. Ortega-Martorell S, Lisboa PJ, Vellido A, Simoes RV, Pumarola M, Julià-Sapé M et al (2012) Convex non-negative matrix factorization for brain tumor delimitation from MRSI data. PLoS ONE 7:e47824
196. Ali AH, Al-hadi SA, Naeemah MR, Mazher AN (2018) Classification of brain lesion using K-nearest neighbor technique and texture analysis. J Phys Conf Ser:012018
197. Supot S, Thanapong C, Chuchart P, Manas S (2007) Segmentation of magnetic resonance images using discrete curve evolution and fuzzy clustering. In: 2007 IEEE International Conference on Integration Technology, pp 697–700
198. Fletcher-Heath LM, Hall LO, Goldgof DB, Murtagh FR (2001) Automatic segmentation of non-enhancing brain tumors in magnetic resonance images. Artif Intell Med 21:43–63
199. Abdulbaqi HS, Mat MZ, Omar AF, Mustafa ISB, Abood LK (2014) Detecting brain tumor in magnetic resonance images using hidden Markov random fields and threshold techniques. In: 2014 IEEE student conference on research and development, pp 1–5
200. Parekh VS, Laterra J, Bettegowda C, Bocchieri AE, Pillai JJ, Jacobs MA (2019) Multiparametric deep learning and radiomics for tumor grading and treatment response assessment of brain cancer: preliminary results, pp 1–6. arXiv:1906.04049
201. Zadeh Shirazi A, Fornaciari E, McDonnell MD, Yaghoobi M, Cevallos Y, Tello-Oquendo L et al (2020) The Application of Deep Convolutional Neural Networks to Brain Cancer Images: A Survey. J Pers Med 10:224
202. Guan B, Yao J, Zhang G, Wang XJPRL (2019) Thigh fracture detection using deep learning method based on new dilated convolutional feature pyramid network 125:521–526
203. Raza M, Sharif M, Yasmin M, Khan MA, Saba T, Fernandes SL (2018) Appearance based pedestrians' gender recognition by employing stacked auto encoders in deep learning. Future Gener Comput Syst 88:28–39
204. Liaqat A, Khan MA, Shah JH, Sharif M, Yasmin M, Fernandes SL (2018) Automated ulcer and bleeding classification from WCE images using multiple features fusion and selection. J Mech Med Biol 18:1850038
205. Naqi S, Sharif M, Yasmin M, Fernandes SL (2018) Lung nodule detection using polygon approximation and hybrid features from CT images. Curr Med Imaging 14:108–117
206. Ansari GJ, Shah JH, Yasmin M, Sharif M, Fernandes SL (2018) A novel machine learning approach for scene text extraction. Futur Gener Comput Syst 87:328–340
207. Fatima Bokhari ST, Sharif M, Yasmin M, Fernandes SL (2018) Fundus image segmentation and feature extraction for the detection of glaucoma: a new approach. Curr Med Imaging 14:77–87
208. Jain VK, Kumar S, Fernandes SL (2017) Extraction of emotions from multilingual text using intelligent text processing and computational linguistics. J Comput Sci 21:316–326
209. Fernandes SL, Gurupur VP, Lin H, Martis RJ (2017) A novel fusion approach for early lung cancer detection using computer aided diagnosis techniques. J Med Imaging Health Inf 7:1841–1850
210. Raja N, Rajinikanth V, Fernandes SL, Satapathy SC (2017) Segmentation of breast thermal images using Kapur's entropy and hidden Markov random field. J Med Imaging Health Inf 7:1825–1829
211. Rajinikanth V, Madhavaraja N, Satapathy SC, Fernandes SL (2017) Otsu's multi-thresholding and active contour snake model to segment dermoscopy images. J Med Imaging Health Inf 7:1837–1840
212. Shah JH, Chen Z, Sharif M, Yasmin M, Fernandes SL (2017) A novel biomechanics-based approach for person re-identification by generating dense color sift salience features. J Mech Med Biol 17:1740011
213. Fernandes SL, Bala GJ (2017) A comparative study on various state of the art face recognition techniques under varying facial expressions. Int Arab J Inf Technol 14:254–259
214. Yasmin M, Sharif M, Mohsin S (2013) Neural networks in medical imaging applications: a survey. World Appl Sci J 22:85–96
215. Chen L, Bentley P, Rueckert D (2017) Fully automatic acute ischemic lesion segmentation in DWI using convolutional neural networks. NeuroImage Clin 15:633–643
216. Abd-Ellah MK, Awad AI, Khalaf AA, Hamed HF (2018) Two-phase multi-model automatic brain tumour diagnosis system from magnetic resonance images using convolutional neural networks. EURASIP J Image Video Process 2018:97
217. Larochelle H, Jodoin P-M (2016) A convolutional neural network approach to brain tumor segmentation. In: Brainlesion: Glioma, multiple sclerosis, stroke and traumatic brain injuries: first international workshop, brainles 2015, Held in Conjunction with MICCAI 2015, Munich, Germany, 5 Oct 5, revised selected papers
218. Kamnitsas K, Ledig C, Newcombe VF, Simpson JP, Kane AD, Menon DK, Rueckert D, Glocker B (2017) Efficient multi-scale 3D CNN with fully connected CRF for accurate brain lesion segmentation. Med Image Anal 36:61–78
219. Dong H, Yang G, Liu F, Mo Y, Guo Y (2017) Automatic brain tumor detection and segmentation using U-Net based fully convolutional networks. In: Annual conference on medical image understanding and analysis, pp 506–517
220. Chen S, Ding C, Liu M (2019) Dual-force convolutional neural networks for accurate brain tumor segmentation. Pattern Recogn 88:90–100
221. Wang Y, Li C, Zhu T, Zhang J (2019) Multimodal brain tumor image segmentation using WRN-PPNet. Comput Med Imaging Graph 75:56–65
222. Amin J, Sharif M, Raza M, Saba T, Sial R, Shad SA (2020) Brain tumor detection: a long short-term memory (LSTM)-based learning model. Neural Comput Appl 32:15965–15973
223. Chelghoum R, Ikhlef A, Hameurlaine A, Jacquir S (2020) Transfer learning using convolutional neural network architectures for brain tumor classification from MRI images. In: IFIP International Conference on Artificial Intelligence Applications and Innovations, pp 189–200
224. Mehrotra R, Ansari MA, Agrawal R, Anand RS (2020) A transfer learning approach for AI-based classification of brain tumors. Mach Learn Appl 2:1–12
225. Zikic D, Ioannou Y, Brown M, Criminisi A (2014) Segmentation of brain tumor tissues with convolutional neural networks. In: Proceedings MICCAI-BRATS, pp 36–39
226. Dvořák P, Menze B (2015) Local structure prediction with convolutional neural networks for multimodal brain tumor segmentation. In: International MICCAI workshop on medical computer vision, pp 59–71
227. Pereira S, Pinto A, Alves V, Silva CA (2016) Brain tumor segmentation using convolutional neural networks in MRI images. IEEE Trans Med Imaging 35:1240–1251
228. Zhao X, Wu Y, Song G, Li Z, Zhang Y, Fan Y (2018) A deep learning model integrating FCNNs and CRFs for brain tumor segmentation. Med Image Anal 43:98–111
229. Hussain S, Anwar SM, Majid M (2018) Segmentation of glioma tumors in brain using deep convolutional neural network. Neurocomputing 282:248–261
230. Sharif MI, Li JP, Amin J, Sharif A (2021) An improved framework for brain tumor analysis using MRI based on YOLOv2 and convolutional neural network. Complex Intell Syst:1–14
231. Kao PY, Shailja S, Jiang J, Zhang A, Khan A, Chen JW, Manjunath BS (2020) Improving patch-based convolutional neural networks

for MRI brain tumor segmentation by leveraging location information. Front Neurosci 13:1–12
232. Ahuja S, Panigrahi B, Gandhi T (2020) Transfer learning based brain tumor detection and segmentation using superpixel technique. In: 2020 International Conference on Contemporary Computing and Applications (IC3A), pp 244–249
233. Rehman A, Naz S, Razzak MI, Akram F, Imran M (2020) A deep learning-based framework for automatic brain tumors classification using transfer learning. Circuits Syst Signal Process 39:757–775
234. Guy-Fernand KN, Zhao J, Sabuni FM, Wang J (2020) Classification of brain tumor leveraging goal-driven visual attention with the support of transfer learning. In: 2020 Information Communication Technologies Conference (ICTC), pp 328–332
235. Kaur T, Gandhi TK (2020) Deep convolutional neural networks with transfer learning for automated brain image classification. Mach Vis Appl 31:1–16
236. Gu Y, Li K (2021) A Transfer Model Based on Supervised Multi-Layer Dictionary Learning for Brain Tumor MRI Image Recognition. Front Neurosci 15:550
237. Sadad T, Rehman A, Munir A, Saba T, Tariq U, Ayesha N et al (2021) Brain tumor detection and multi-classification using advanced deep learning techniques. Microsc Res Tech 84:1296–1308
238. Panwar SA, Munot MV, Gawande S, Deshpande PS (2021) A reliable and an efficient approach for diagnosis of brain tumor using transfer learning. Biomed Pharmacol J 14:283–294
239. Kumar RL, Kakarla J, Isunuri BV, Singh M (2021) Multi-class brain tumor classification using residual network and global average pooling. Multimedia Tools Appl 80:13429–13438
240. Arbane M, Benlamri R, Brik Y, Djerioui M (2021) Transfer learning for automatic brain tumor classification using MRI images. In: 2020 2nd International Workshop on Human-Centric Smart Environments for Health and Well-being (IHSH), pp 210–214
241. Amin J, Sharif M, Yasmin M, Saba T, Anjum MA, Fernandes SL (2019) A new approach for brain tumor segmentation and classification based on score level fusion using transfer learning. J Med Syst 43:1–16
242. Wu W, Chen AY, Zhao L, Corso JJ (2014) Brain tumor detection and segmentation in a CRF (conditional random fields) framework with pixel-pairwise affinity and superpixel-level features. Int J Comput Assist Radiol Surg 9:241–253
243. Noreen N, Palaniappan S, Qayyum A, Ahmad I, Imran M, Shoaib M (2020) A deep learning model based on concatenation approach for the diagnosis of brain tumor. IEEE Access 8:55135–55144
244. Zhang J, Jiang Z, Dong J, Hou Y, Liu B (2020) Attention gate resU-Net for automatic MRI brain tumor segmentation. IEEE Access 8:58533–58545
245. Rehman ZU, Zia MS, Bojja GR, Yaqub M, Jinchao F, Arshid K (2020) Texture based localization of a brain tumor from MR-images by using a machine learning approach. Med Hypotheses 141:109705
246. Zeineldin RA, Karar ME, Coburger J, Wirtz CR, Burgert O (2020) DeepSeg: deep neural network framework for automatic brain tumor segmentation using magnetic resonance FLAIR images. Int J Comput Assist Radiol Surg 15:909–920
247. Swati ZNK, Zhao Q, Kabir M, Ali F, Ali Z, Ahmed S et al (2019) Content-based brain tumor retrieval for MR images using transfer learning. IEEE Access 7:17809–17822
248. Pravitasari AA, Iriawan N, Almuhayar M, Azmi T, Fithriasari K, Purnami SW et al (2020) UNet-VGG16 with transfer learning for MRI-based brain tumor segmentation. Telkomnika 18:1310–1318
249. Deepak S, Ameer P (2019) Brain tumor classification using deep CNN features via transfer learning. Comput Biol Med 111:3345
250. Lu S, Lu Z, Zhang Y-D (2019) Pathological brain detection based on AlexNet and transfer learning. J Comput Sci 30:41–47
251. Wacker J, Ladeira M, Nascimento JEV (2019) Transfer learning for brain tumor segmentation. arXiv:1912.12452
252. Soumik MFI, Hossain MA (2020) Brain tumor classification with inception network based deep learning model using transfer learning. In: 2020 IEEE Region 10 Symposium (TENSYMP), pp 1018–1021
253. Khamparia A, Gupta D, de Albuquerque VHC, Sangaiah AK, Jhaveri RH (2020) Internet of health things-driven deep learning system for detection and classification of cervical cells using transfer learning. J Supercomput 76:1–19
254. Yang Y, Yan LF, Zhang X, HanY, Nan HY, Hu YC, Hu B, Yan SL, Zhang J, Cheng DL, Ge XW (2018) Glioma grading on conventional MR images: a deep learning study with transfer learning. Front Neurosci 12:1–10
255. Banerjee S, Mitra S, Masulli F, Rovetta S (2019) Deep radiomics for brain tumor detection and classification from multi-sequence MRI. arXiv:1903.09240
256. Hao R, Namdar K, Liu L, Khalvati F (2021) A transfer learning–based active learning framework for brain tumor classification. Front Artif Intell 4
257. Saxena P, Maheshwari A, Maheshwari S (2021) Predictive modeling of brain tumor: a deep learning approach. In: Innovations in computational intelligence and computer vision, pp 275–285
258. Bergholm V, Izaac J, Schuld M, Gogolin C, Alam MS, Ahmed S et al (2018) Pennylane: automatic differentiation of hybrid quantum-classical computations. arXiv:1811.04968
259. Zhou R, Zhou L, Jiang N, Ding Q (2006) Dynamic analysis and application of QANN. In: First International Multi-Symposiums on Computer and Computational Sciences (IMSCCS'06), pp 347–351
260. Li P, Xiao H (2014) Sequence input-based quantum-inspired neural networks with applications. Neural Process Lett 40:143–168
261. Konar D, Bhattacharyya S, Panigrahi BK, Behrman EC (2021) Qutrit-inspired fully self-supervised shallow quantum learning network for brain tumor segmentation. IEEE Trans Neural Netw Learn Syst
262. Agrawal U, Brown EN, Lewis LD (2020) Model-based physiological noise removal in fast fMRI. Neuroimage 205:1–18
263. Dubey YK, Mushrif MM (2016) FCM clustering algorithms for segmentation of brain MR images. Adv Fuzzy Syst 2016:8
264. Sharif MI, Khan MA, Alhussein M, Aurangzeb K, Raza M (2021) A decision support system for multimodal brain tumor classification using deep learning. Complex Intell Syst:1–14
265. Irshad M, Muhammad N, Sharif M, Yasmeen M (2018) Automatic segmentation of the left ventricle in a cardiac MR short axis image using blind morphological operation. Eur Phys J Plus 133:1–14
266. Han C, Rundo L, Araki R, Furukawa Y, Mauri G, Nakayama H et al (2020) Infinite brain MR images: PGGAN-based data augmentation for tumor detection. Neural approaches to dynamics of signal exchanges. Springer, New York, pp 291–303
267. Juan-Albarracín J, Fuster-Garcia E, Manjon JV, Robles M, Aparici F, Martí-Bonmatí L et al (2015) "Automated glioblastoma segmentation based on a multiparametric structured unsupervised classification. PLoS ONE 10:e0125143
268. Soltaninejad M, Yang G, Lambrou T, Allinson N, Jones TL, Barrick TR et al (2018) "Supervised learning based multimodal MRI brain tumour segmentation using texture features from supervoxels. Comput Methods Progr Biomed 157:69–84
269. Ito KL, Kim H, Liew SL (2019) A comparison of automated lesion segmentation approaches for chronic stroke T1-weighted MRI data. Hum Brain Mapp 40:4669–4685
270. Chen X, You S, Tezcan KC, Konukoglu EJMIA (2020) Unsupervised lesion detection via image restoration with a normative prior

271. Liu P, Dou Q, Wang Q, Heng PA (2020) An encoder-decoder neural network with 3D squeeze-and-excitation and deep supervision for brain tumor segmentation. IEEE Access 8:34029–34037
272. Deb D, Roy S (2021) Brain tumor detection based on hybrid deep neural network in MRI by adaptive squirrel search optimization. Multimedia Tools Appl 80:2621–2645
273. Feng X, Tustison NJ, Patel SH, Meyer CH (2020) "Brain tumor segmentation using an ensemble of 3d u-nets and overall survival prediction using radiomic features. Front Comput Neurosci 14:25
274. Zhou C, Ding C, Wang X, Lu Z, Tao D (2020) "One-pass multi-task networks with cross-task guided attention for brain tumor segmentation. IEEE Trans Image Process 29:4516–4529